IOPscience iopscience.iop.org

Home Search Collections Journals About Contact us My IOPscience

Mössbauer spectroscopy as a probe of silicate glasses

This article has been downloaded from IOPscience. Please scroll down to see the full text article.

2005 J. Phys.: Condens. Matter 17 R381

(http://iopscience.iop.org/0953-8984/17/8/R01)

View the table of contents for this issue, or go to the journal homepage for more

Download details:
IP Address: 129.252.86.83
The article was downloaded on 27/05/2010 at 20:22

Please note that terms and conditions apply.

INSTITUTE OF PHYSICS PUBLISHING JOURNAL OF PHYSICS: CONDENSED MATTER

J. Phys.: Condens. Matter **17** (2005) R381–R412 doi:10.1088/0953-8984/17/8/R01

TOPICAL REVIEW

Mössbauer spectroscopy as a probe of silicate glasses

J A Johnson[1] **and C E Johnson**[2]

[1] Energy Technology Division, Argonne National Laboratory, Argonne, IL 60439, USA
[2] Physics Department, Northern Illinois University, DeKalb, IL 60115, USA

Received 10 November 2004, in final form 17 December 2004
Published 11 February 2005
Online at stacks.iop.org/JPhysCM/17/R381

Abstract

Mössbauer spectroscopy of tin and iron has been used to probe silicate glasses. The research was motivated by the need to understand the structure and behaviour of float glass when tin diffuses into the surface during manufacture. Iron is also present in small quantities as it is an impurity in the sand from which the glass is made, and it is known to affect the tin uptake. Because float glass is a complex mixture of silica and several modifier oxides, Mössbauer spectroscopy on simpler systems containing silica and a single alkali or alkaline earth modifier has been carried out first to facilitate the interpretation of the data. The spectra have broad lines, reflecting the large number of different sites in an atomically disordered material. Several conclusions were reached from a review of the literature on silicate glasses. The isomer shifts and quadrupole splittings identify the ionic states of the Mössbauer atoms, and the changes when the composition is varied by adding modifier atoms are due to small changes in the local structure and atomic volume. It appears that Sn^{2+} and Fe^{3+} act as conditional glass formers in silicate glasses, while Sn^{4+} and Fe^{2+} are modifiers. From measurements of the relative areas of Sn^{2+} and Sn^{4+} in the Mössbauer spectrum of sectioned specimens, the depth profiles of each oxidation state were determined separately. By monitoring the oxidation of Sn^{2+} to Sn^{4+} produced by heat treatment in air, the diffusion coefficient of oxygen was determined. Measurements on tinted float glass containing several per cent of iron show that the iron and tin react with each other, the Fe^{3+} oxidizing the Sn^{2+} to Sn^{4+}. By combining these data with the depth profiles, a flow diagram of the chemical reactions in the float-glass process has been proposed.

Contents

 © 2005 IOP Publishing Ltd Printed in the UK

1. Introduction

Glassy materials, whether man made or naturally occurring, have been recognized for centuries, though attempts to understand their nature are relatively recent [1]. They are produced by rapidly cooling the constituent materials after melting, and are non-crystalline. Unlike crystalline materials, which have a periodic structure that may be determined by diffraction techniques, there is no direct way of determining the arrangement of atoms in glasses. Their diffraction patterns consist of diffuse rings, from which the radial distribution function of atoms may be deduced. Indeed, unlike crystals, which have a unique three-dimensional structure depending on their composition, temperature and pressure, a glass does not have a unique structure, but it depends upon the conditions under which it was formed, principally the rate at which it was cooled through the glass transition point. Hence, spectroscopic techniques such as Mössbauer spectroscopy, nuclear magnetic resonance and nuclear quadrupole resonance can play an important part in complementing diffraction measurements.

Glasses have short-range atomic order but no long-range order, which only exists in crystals. The glass transition is a second-order change with a discontinuity in the slope of the volume versus temperature curve but not in the volume itself. The glass transition temperature (T_g) may be determined by differential thermal analysis (DTA). For a crystal, solidification is a first-order change with a sharp discontinuity in the volume. In forming a glass the material may be supercooled below the melting point. The free energy of the material is higher in the glassy (disordered) state than in the crystalline (ordered) state. Hence thermodynamically the crystal is a stable state. However, a glass has strong directional covalent bonds which must be broken in order to be converted to a crystal, which is more ionic. Hence the time taken for a glass to reach its equilbrium crystalline state may be infinite for all practical purposes.

Only certain materials may form glasses. The oxides which form glasses ('network formers') include SiO_2, B_2O_3, GeO_2, P_2O_5 and As_2O_3 and are characterized by strong covalent bonding. Some other oxides, e.g. Al_2O_3, are not network formers by themselves, but they do not weaken the bonding in the network and are known as 'intermediates'. Finally, the strongly ionic oxides, e.g. Na_2O, K_2O and CaO, do not form glasses themselves and weaken the bonding when incorporated in a glass network; they are known as 'network modifiers'.

It is not possible to predict in all cases whether the added atoms will behave as network formers (substitutional, tetrahedrally co-ordinated, covalently bonded) or as modifiers (interstitial, octahedrally co-ordinated, ionically bonded) or as intermediates. There is a basic

scientific and technical need to establish the specific structural changes brought about by the incorporation of modifiers, and how these changes affect the properties of the glasses. For many years the glass network was thought to be completely random. Recently both theoretical and experimental research has suggested otherwise [2]. Spectroscopic techniques (including Mössbauer spectroscopy) have a valuable contribution to make here.

The glasses discussed in this article are transparent silicate glasses. They are based on silica, SiO_2, which in its crystalline state contains silicon tetrahedrally co-ordinated to oxygen. In glasses the SiO_4 tetrahedra are still present, and each oxygen bridges two such tetrahedra, but neighbouring tetrahedra are no longer arranged in a fixed orientation with respect to each other.

Pure SiO_2 has a high melting point ($T_m = 2003$ K) and glass transition temperature ($T_g = 1453$ K). In optical glass manufacture several other oxides, mainly network modifiers, are added to the SiO_2 to reduce these and to improve the properties of the resulting glass e.g. reducing the viscosity in the liquid state. Usually Na_2O is added to lower the melting point and CaO to increase the durability. The addition of small amounts of Na_2O results in the Na^+ ions fitting the interstitial sites with (approximate) octahedral co-ordination in the network and, to keep the charge neutral, the formation of two non-bridging oxygen ions (O^-) per sodium atom, thus breaking the network structure. If too large an amount of Na_2O is added the glass will crystallize. Another additive is Al_2O_3, which is an intermediate, i.e. it may either substitute for silicon with tetrahedral co-ordination or may enter interstitially with octahedral co-ordination.

2. Float glass

Float glass is the result of a search for a method to manufacture sheets of flat glass directly without the expense of subsequently grinding it to size. The process utilizes the surface of a liquid as a readily available, convenient and reproducible flat surface. The idea is to float a moving ribbon of molten glass on a bath of molten tin in a reducing atmosphere. The glass is at a temperature of 600 °C, well above the tin melting point of 280 °C. Getting the conditions right to make the process continuous on a large scale was a formidable task and was the brainchild of Alistair (later Sir Alistair) Pilkington. The story of the invention is an interesting one [3] and is a lesson in perseverance and management in research. After many years of development without success, the company he worked for (Pilkingtons—same name, but no family connection) gave him another six months to prove he could get the process to work. During that time he ran the first successful plant, and within a few years virtually all the flat glass in the world was produced by this process.

Float glass is a complex material composed of several oxides. A typical composition is silicon (73%), sodium (11%), calcium (8%), magnesium (6%), aluminium (0.5%), potassium (0.3%), and iron (0.05%) as well as the tin that has diffused in from the bath. Sodium is added to lower the melting point, calcium and magnesium harden the surface, while iron is an impurity in the sand from which the float glass is made.

In spite of its widespread use several poorly understood features in float glass manufacture need to be studied. During the process some tin inevitably diffuses into the bottom surface of the glass, which is in contact with the molten tin. Some tin also diffuses into the top surface since tin atoms are present in the atmosphere above the bath. The presence of tin, as well as the variability of its oxidation state, changes the physical (refractive index, thermal expansion coefficient, viscosity etc) and chemical properties. These effects can become significant during secondary processing such as chemical toughening or thermal treatment. For example, because the process takes place in a reducing atmosphere the tin enters the glass in the Sn^{2+} state, and its subsequent oxidation to Sn^{4+} causes a wrinkling of the surface ('bloom') and hence a deterioration of the optical clarity. Understanding the structure is important and Mössbauer

spectroscopy is a convenient and non-destructive method for examining the oxidation state and measuring the chemical binding. None of the major constituents is a Mössbauer isotope, but iron and tin are important ingredients in commercial surface coatings and glazes, and tin diffuses into the surface in the float glass process, so many spectroscopy studies have been done using ^{57}Fe and ^{119}Sn.

3. Mössbauer spectroscopy

Mössbauer spectroscopy yields information on the chemical state, coordination number and symmetry of the ligands of atoms containing a Mössbauer nucleus. It complements neutron scattering, which measures the (average) bond lengths and coordination numbers of all the atoms. Many industrially relevant questions have been answered about the role of tin and other atoms in float glass, i.e., are they modifiers (break up the glass network), formers (participate in the glass network) or intermediates (form a glass under certain conditions)?

Spectra may be measured in transmission or by scattering (fluorescence). Measuring conversion electrons (conversion electron Mössbauer spectroscopy or CEMS) yields information specific to the surface, and has been used to establish the depth profiles of the tin in float glass.

The hyperfine interactions in the Mössbauer spectrum have several features which provide information on the state of the atoms. The isomer shift and, to a lesser extent, the quadrupole splitting can determine the ionization state and the degree of covalency. The quadrupole splitting is sensitive to the symmetry of the ligand environment of the Mössbauer atom. The probability of the Mössbauer effect, the f-factor, determines the strength of the interatomic forces. Both the shift and the f-factor can be used to infer the co-ordination number of the Mössbauer atom.

Numerous measurements have already been made of the Mössbauer spectra of glasses, and an extensive literature now exists on the subject. Earlier results have been summarized and references given in review articles by Kirkjian [4], Coey [5], Müller-Warmuth and Eckert [6], Tomandl [7], Nishida [8] and others.

In this paper we shall review Mössbauer measurements on silicate glasses. The spectra enable the relative abundance and binding strength of different oxidation states (e.g. Sn^{2+} and Sn^{4+}) to be compared. Measurements of the dependence of the chemical (isomer) shift on composition and temperature enable changes in the glass, due to the presence of modifiers, to be studied.

We now consider the main features of the Mössbauer spectrum and how they are used in the study of glasses.

3.1. Linewidth

The lines in the Mössbauer spectra of glasses are broad, as expected for a disordered material, where the atoms are in different environments, each with slightly different isomer shifts and quadrupole splittings. This observation was made for the first Mössbauer spectrum of ^{57}Fe in an amorphous material (fused quartz), by Pollack *et al* [9]. This spectrum also showed that the Mössbauer effect is not restricted to crystals, although the theory of the effect is based on the properties of phonons in a crystalline lattice.

3.2. Centre shift

The position δ of the centroid of the Mössbauer spectrum depends upon the temperature through the second-order Doppler shift δ^{SOD} and on the chemical state of the atom containing

the Mössbauer nucleus via the isomer shift δ^{I}. Thus

$$\delta = \delta^{\mathrm{SOD}} + \delta^{\mathrm{I}}. \tag{1}$$

These contributions may be separated since the variation of δ^{SOD} with temperature may be calculated; whence δ^{I} may be deduced.

3.2.1. Second-order Doppler shift. The second-order Doppler shift δ^{SOD} is a relativistic change in the γ-ray energy arising from the motion of the Mössbauer nucleus and is given by

$$\delta^{\mathrm{SOD}} = -\frac{1}{2}\frac{\langle v^2\rangle}{c} = -\frac{U}{2Mc} \tag{2}$$

where v is the velocity of the nuclei and c is the velocity of light. U is the internal energy per atom and M is its mass. It is given according to the Debye model by

$$\delta = -\frac{9}{2}\frac{k\Theta_{\mathrm{D}}}{Mc}\left[\frac{1}{8} + \left(\frac{T}{\Theta_{\mathrm{D}}}\right)^4 \int_0^{\theta_{\mathrm{D}/T}} \frac{x^3}{\mathrm{e}^x - 1}\mathrm{d}x\right] \tag{3}$$

where Θ_{D} is the Debye temperature, k is Boltzmann's constant and T is the temperature. The value of δ^{SOD} becomes more negative as the temperature is increased. At high temperatures ($T > \Theta_{\mathrm{D}}$) δ^{SOD} is independent of Θ_{D} and is linear with temperature according to

$$\delta^{\mathrm{SOD}} = -3kT/2Mc. \tag{4}$$

At low temperatures ($T < \Theta_{\mathrm{D}}$) the data could be used in principle to give an estimate of Θ_{D}, but not as accurately as from measurements of the f-factor (see section 3.5).

The Debye temperature is used here as a convenient parameter for comparing the binding strength of the Mössbauer atoms. It is not meant to imply that the Debye model is valid for glasses.

3.2.2. Isomer shift. The isomer (or chemical) shift gives a measure of the s-electron density at the Mössbauer nuclei and is given by

$$\delta^{\mathrm{I}} = \tfrac{2}{3}\pi Ze^2\Delta\langle R^2\rangle\Delta\rho_{\mathrm{s}}\,(0) \tag{5}$$

where $\Delta\langle R^2\rangle$ is the change in the mean square nuclear radius in the Mössbauer transition, $\Delta\rho_{\mathrm{s}}(0)$ is the difference between the electron densities at the Mössbauer nuclei in the source and absorber and Ze is the nuclear charge. Hence δ^{I} is sensitive to the charge state and covalency of the Mössbauer atom and may be used to assign its co-ordination number. Thus the isomer shift is an important parameter in determining the local structure in a glass. It has to be calibrated for each Mössbauer isotope. Although the effects of covalency and co-ordination number on the isomer shift are well known to Mössbauer spectroscopists, we outline here the main features for the two most frequently used isotopes, ^{57}Fe and ^{119}Sn.

Since δ^{I} depends upon the density, i.e. it is inversely proportional to the molar volume, its variation with temperature is given using Gruneisen's law that the expansivity is proportional to the specific heat by

$$\delta^{\mathrm{I}}(T) = \delta^{\mathrm{I}}(0)[1 - \beta_\infty U/3k] \tag{6}$$

where β_∞ is the expansivity at high temperatures (e.g. room temperature).

3.3. Quadrupole splitting

The quadrupole splitting measures the electric field gradient at the nucleus, and increases as the molar volume decreases or as the arrangement of the ligands becomes more asymmetric.

For Sn^{2+} the dominant contribution to the electric field gradient comes from the 5p electrons, and the quadrupole splitting is given by

$$\Delta = \tfrac{2}{5}e^2 Q\langle r^{-3}\rangle_{5p}\langle 3\cos^2\theta - 1\rangle_{5p} \tag{7}$$

where Q is the electric quadrupole moment of the nuclei and r is the radial co-ordinate of the electrons. When the temperature is increased $\langle r^{-3}\rangle_{5p}$ decreases due to thermal expansion and hence Δ decreases as observed. With Gruneisen's assumption that the expansivity is proportional to the specific heat, the predicted temperature variation is

$$\Delta(T) = \Delta(0)[1 - \beta_\infty U/3k]. \tag{8}$$

3.4. Magnetic hyperfine splitting

The ^{57}Fe Mössbauer spectrum may be split into six lines by the hyperfine magnetic field in magnetically ordered materials or in dilute paramagnets. Most iron-containing silicate glasses show a splitting of the Fe^{3+} spectrum at low temperatures where spin–lattice relaxation is slow. The hyperfine fields are about 50 T. At higher temperatures the lines broaden and eventually coalesce into two quadrupole-split lines.

3.5. f-factor

The recoil-free fraction (f-factor) is given in the harmonic approximation by

$$f = \exp(-\kappa^2\langle x^2\rangle) \tag{9}$$

where κ is the wavenumber of the γ-ray and $\langle x^2\rangle$ is the mean square displacement of the atom from its equilibrium position.

In the Debye model, the recoil-free fraction, f, is related to the Debye temperature, Θ_D, and the nuclear recoil energy, E_R, via the equation

$$\ln f = -\frac{3}{2}\frac{E_R}{k\Theta_D}\left(1 + 4\left(\frac{T}{\Theta_D}\right)^2\int_0^{\Theta_D/T}\frac{x}{e^x - 1}\,dx\right). \tag{10}$$

At high temperatures ($T > \Theta_D/2$),

$$\frac{d}{dT}(\ln f) = -\frac{6E_R}{k\Theta_D^2}. \tag{11}$$

Θ_D may be found from fitting the decrease in absorption area with temperature to equations (10) or (11).

The Debye temperature gives a measure of the strength of the atomic binding, and may be different in different oxidation states. To estimate the relative abundance of two oxidation states from their contributions to the Mössbauer spectra it is necessary to determine Θ_D for each of them. Breaking the glass network by the addition of modifiers decreases the atomic vibrational frequencies and hence Θ_D.

4. Glasses containing iron

In 1961 Pollack *et al* [9] presented the first Mössbauer spectra of glasses at the First International Conference on the Applications of the Mössbauer Effect in Paris. They measured ^{57}Fe in fused

quartz and Pyrex. Since then an enormous amount of work has been done on silicate and other glasses. Traces of iron are always present in commercial glasses and arise from impurities in the sand from which they are made. Iron is also added in concentrations up to 5 mol% Fe_2O_3 to produce tinted glass to reduce infra-red transmission for use in solar-control glazing. Many naturally occurring silicate minerals are in the glassy state. An extensive review of data on iron in inorganic glasses has been given by Dyar [10].

Early work by Kirkjian and Buchanan [11], Gosselin *et al* [12] and Levy *et al* [13] established that both Fe^{3+} and Fe^{2+} are present in varying amounts depending upon the method of preparation, and that Fe^{2+} behaves as a network modifier occupying predominantly octahedral sites while Fe^{3+} is a network former occupying tetrahedral sites. Levy *et al* [13] found that the replacement by CaO of sodium atoms in sodium iron silicate glasses increases the isomer shift and quadrupole splitting for both valence states of iron.

More recently, Johnson *et al* [14] combined Mössbauer spectroscopy with neutron diffraction to study iron sodium silicate glasses with the composition $(Fe_2O_3)_x(Na_2O)_{0.3}(SiO_2)_{0.7-x}$. Williams *et al* [15] made similar measurements on specimens of float glass which had been re-melted with Fe_2O_3 and on tinted float glass, i.e. glass in which Fe_2O_3 had been added to the float plant charge [16, 17]. Hayashi *et al* [18] made measurements on iron silicate glasses with mixtures of sodium and calcium modifiers in a study of relaxation after heating toward equilibrium. Bingham *et al* [19] studied iron in soda-lime silicate glasses and found evidence for iron clustering.

Some typical spectra are plotted in figure 1 and are seen to be a superposition of an Fe^{3+} and an Fe^{2+} doublet, which are distinguishable by their chemical shifts. The majority of the iron was in the Fe^{3+} state, with between 7 and 15% being Fe^{2+}, the proportion of Fe^{2+} being less for samples with higher total iron content. The lines were broad (full width at half maximum $\sim$0.6 mm s^{-1} compared to the natural width of 0.19 mm s^{-1}) corresponding to the distribution of local environments, which is characteristic of glasses.

The low values of the shift of the majority Fe^{3+} ions ($\sim$0.27 mm s^{-1} at 297 K) indicate that the iron is four coordinate. Typical values for Fe^{3+} tetrahedrally coordinated to oxygen in silicate glasses are in the range 0.20–0.32 mm s^{-1}, compared with 0.35–0.55 mm s^{-1} for octahedral coordination [10]. This finding suggests that ferric iron substitutes for silicon, i.e. it behaves as a conditional glass former. For Fe^{2+} typical values are 0.90–0.95 mm s^{-1} (tetrahedral) and 1.05–1.10 mm s^{-1} (octahedral) [10], so the observed shift (1.02 mm s^{-1} at 297 K) is consistent with an average coordination number of about five. However, there is a large uncertainty for the Fe^{2+} data owing to the small amounts present. The neutron data confirm that the iron is four coordinate and indicate that the Fe–O bond lengths are about 1.90 Å and the O–Fe–O bond angles approach 90°. The Fe–O bond length decreases and the O–O bond length increases with increasing Fe_2O_3 content.

These assignments agree with previous Mössbauer work of Hirao *et al* [20] and Ramachandran and Balasubramanian [21], but disagree with conclusions of Iwamoto *et al* [22] from extended x-ray absorption fine structure measurements. Frischat and Tomandl [23] suggested that the Fe^{3+} coordination number depends upon the iron concentration, but no evidence to support this hypothesis has been found.

Table 1 lists the centre shifts (δ) and quadrupole splittings (Δ) measured at 77 K for several iron silicate glasses. Some authors [13, 16] fit the Fe^{3+} spectrum with separate components for tetrahedral and octahedral co-ordination, while others [12, 14, 15] fit the spectra to give an average value for the isomer shift and quadrupole splitting. Both are given in the table. Values for ternary sodium stannosilicate glasses are plotted as a function of iron content in figure 2.

It is seen that for both Fe^{3+} and Fe^{2+} δ decreased while Δ increased as the iron concentration was increased. These changes are small and are due to changes in the isomer shift δ^{I}. The data

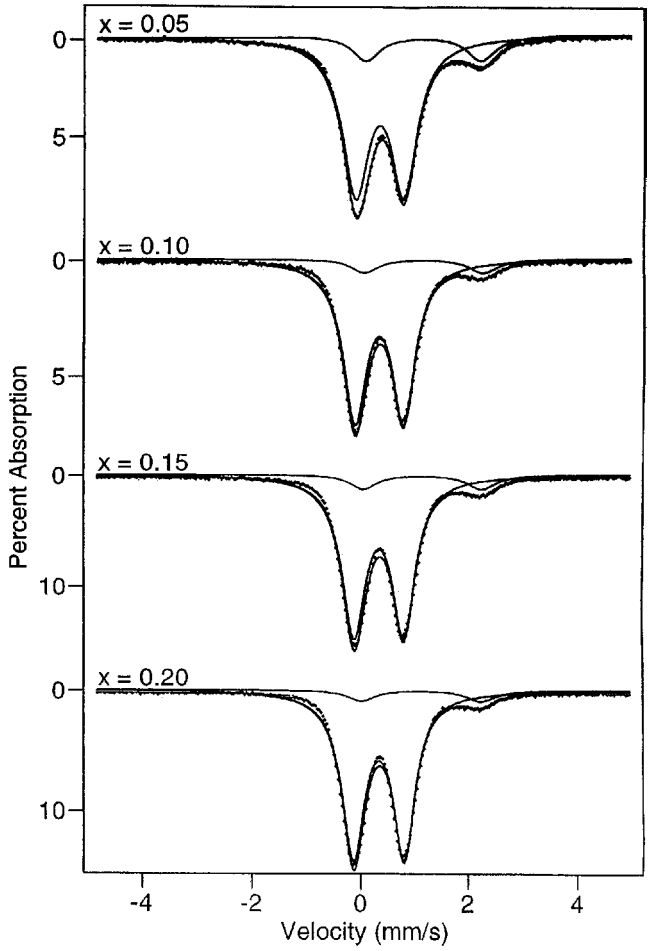

Figure 1. Mössbauer spectra at 77 K of ^{57}Fe in $(Fe_2O_3)_x(Na_2O)_{0.3}(SiO_2)_{0.7-x}$ glasses [14].

of figure 2 give

$$\partial\delta^{\mathrm{I}}/\partial c = -0.28 \text{ mm s}^{-1} \text{ mol}^{-1} \tag{12}$$

and

$$\partial\Delta/\partial c = +0.393 \text{ mm s}^{-1} \text{ mol}^{-1}. \tag{13}$$

Since the molar volume decreases as iron is added, the decrease in s-electron density at the nucleus is evidence for screening by the d electrons. This conclusion is supported by the increase in asymmetry shown by the increase in quadrupole splitting. The shift in the Mössbauer spectra with temperature was less than that predicted for the second-order Doppler shift, showing an intrinsic temperature dependence of the isomer shift, consistent with thermal expansion.

The decrease in the Mössbauer fraction as the temperature increased is shown in figure 3. The effect in Fe^{2+} falls off more quickly with temperature than in Fe^{3+}. The effective Debye temperatures were determined to be 312 K for Fe^{3+} and 268 K for Fe^{2+}. As the Debye temperature is proportional to the binding strength, this shows that Fe^{3+} is more tightly bound

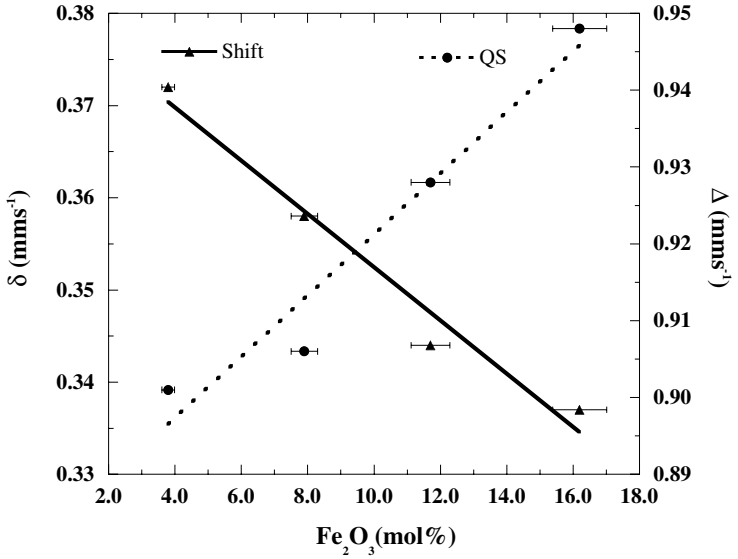

Figure 2. Variation of the ^{57}Fe shift δ (▲ and solid line) and quadrupole splitting Δ (● and dashed line) of Fe^{3+} with Fe_2O_3 concentration [14].

Table 1. Shifts (δ) and quadrupole splittings (Δ) of ^{57}Fe in silicate glasses.

	Fe^{2+}		Fe^{3+} Octahedral		Fe^{3+} Tetrahedral			
	δ	Δ	δ	Δ	δ	Δ	T (K)	Ref.
$(Float)(Fe_2O_3)_{0.002}$	1.166	2.09			0.25	0.9	4.2	[15]
$(Float)(Fe_2O_3)_{0.003}$	1.157	2.09			0.33	0.9	4.2	[15]
$(Float)(Fe_2O_3)_{0.008}$	1.113	2.14			0.4	0.935	4.2	[15]
$(Float)(Fe_2O_3)_{0.015}$	1.107	2.22			0.42	0.89	4.2	[15]
$(Float)(Fe_2O_3)_{0.029}$	1.1	2.16			0.37	0.95	4.2	[15]
$(Float)(Fe_2O_3)_{0.040}$	1.1	2.24			0.38	0.96	4.2	[15]
$(SiO_2)_{0.59}(Na_2O)_{0.20}(Fe_2O_3)_{0.21}$	1.14	2.08			0.4	0.87	RT	[12]
$(SiO_2)_{0.41}(Na_2O)_{0.14}(Fe_2O_3)_{0.45}$	1.08	2.22			0.34	0.88	RT	[12]
$(SiO_2)_{0.65}(Na_2O)_{0.30}(Fe_2O_3)_{0.05}$	1.184	2.142			0.372	0.901	77	[14]
$(SiO_2)_{0.60}(Na_2O)_{0.30}(Fe_2O_3)_{0.10}$	1.177	2.205			0.358	0.906	77	[14]
$(SiO_2)_{0.55}(Na_2O)_{0.30}(Fe_2O_3)_{0.15}$	1.151	2.194			0.344	0.928	77	[14]
$(SiO_2)_{0.50}(Na_2O)_{0.30}(Fe_2O_3)_{0.20}$	1.122	2.22			0.337	0.948	77	[14]
$(SiO_2)_{0.58}(Na_2O)_{0.38}(Fe_2O_3)_{0.04}$	0.99	1.97			0.25	0.86	RT	[16]
$(SiO_2)_{0.48}(Na_2O)_{0.32}(Fe_2O_3)_{0.20}$	0.77	2.43	0.23	0.74	0.23	1.14	RT	[16]
$(SiO_2)_{0.42}(Na_2O)_{0.23}(Fe_2O_3)_{0.35}$	0.93	2.43	0.39	0.72	0.4	1.13	RT	[13]
$(SiO_2)_{0.29}(Na_2O)_{0.36}(Fe_2O_3)_{0.35}$	0.91	2.46	0.36	0.62	0.36	1.04	RT	[13]
$(SiO_2)_{0.58}(CaO)_{0.38}(Fe_2O_3)_{0.04}$	1.03	1.96			0.31	1.16	RT	[16]
$(SiO_2)_{0.40}(CaO)_{0.40}(Fe_2O_3)_{0.20}$	0.75	2.33	0.22	0.87	0.19	1.47	RT	[16]
$(SiO_2)_{0.48}(CaO)_{0.32}(Fe_2O_3)_{0.20}$	0.75	2.28	0.25	0.86	0.21	1.49	RT	[16]
$(SiO_2)_{0.42}(CaO)_{0.23}(Fe_2O_3)_{0.35}$	0.88	2.53	0.5	0.85	0.48	1.39	RT	[13]
$(SiO_2)_{0.29}(CaO)_{0.36}(Fe_2O_3)_{0.35}$	0.82	2.52	0.46	0.91	0.44	1.52	RT	[13]

than Fe^{2+}, as expected from its higher charge. These data have to be used to correct the observed fractions of the two ionic states in the spectrum to obtain the actual relative amounts present.

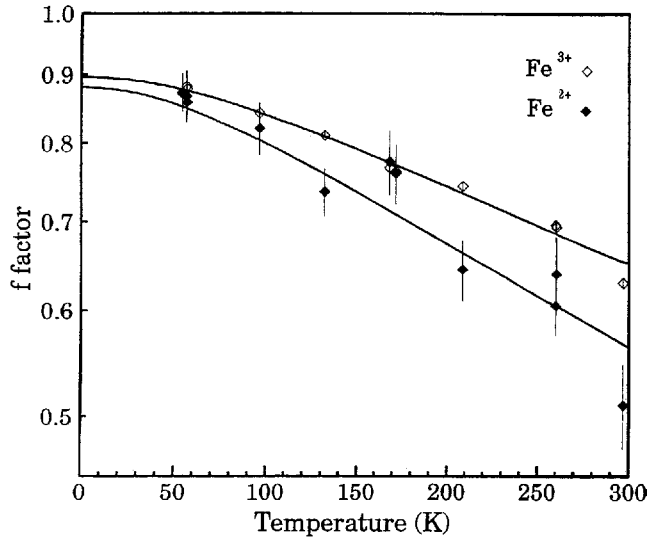

Figure 3. Temperature variation of the f-factors of Fe^{3+} and Fe^{2+} for $(Fe_2O_3)_{0.05}(Na_2O)_{0.3}(SiO_2)_{0.65}$. The solid curves are fits with $\Theta_D \sim 312$ K (Fe^{3+}) and $\Theta_D \sim 268$ K (Fe^{2+}) [14].

Most silicate glasses containing iron are not ordered magnetically. An exception is $(SiO_2)_{0.66}(Al_2O_3)_{0.16}(Fe_2O_3)_{0.11}(K_2O)_{0.07}$, where the Mössbauer spectra [24] show magnetic hyperfine interaction, indicating the presence of a crystalline magnetite-like phase dispersed in a glassy matrix. However, in most glasses containing low concentrations (up to a few per cent) of iron the Fe^{3+} spectrum shows magnetic splitting as in figure 4 [15]. At 4.2 K the magnetic splitting is fully resolved, corresponding to a hyperfine field of about 51 T (figure 4(c)). The Fe^{2+} spectrum is not magnetic. At room temperature (figure 4(b)) the faster electron spin relaxation broadens the Fe^{3+} spectrum. Comparison with figure 4(a) illustrates the necessity of making measurements over a large velocity range in order to estimate accurately the intensity of the Fe^{3+} contribution to the spectrum.

5. Glasses containing tin

When tin is incorporated into pure silica it occurs as Sn^{2+}, Sn^{4+} being insoluble. However, in the presence of modifiers (e.g. Na^+, Ca^{2+}) Sn^{4+} becomes soluble, so that in float glass both ionic states may occur. The co-existence of Sn^{2+} and Sn^{4+} in amorphous and glassy materials has been demonstrated from ^{119}Sn Mössbauer spectra. Collins *et al* [25] made such measurements on amorphous tin oxides. Silicate glasses containing various modifiers have been analysed by several groups. In early work Dannheim *et al* [26] studied the effects of Na and Al, and Mitrofanov and Sidorov [27] studied the alkali modifiers Li, Na and K.

To study tin in a complex material like float glass, it is useful to start with simpler systems first. The simplest system is the binary glass composed only of oxides of tin and silicon studied by Williams *et al* in 1995 [28]. Next, float glass doped with tin oxide and re-melted was investigated [29] to improve the Mössbauer signal and was shown to be a good model for undoped float glass. Once the technique had been established as a useful tool to study these materials, research was expanded to ternary glasses made up of various combinations of the float glass components. Johnson *et al* carried out Mössbauer and neutron scattering

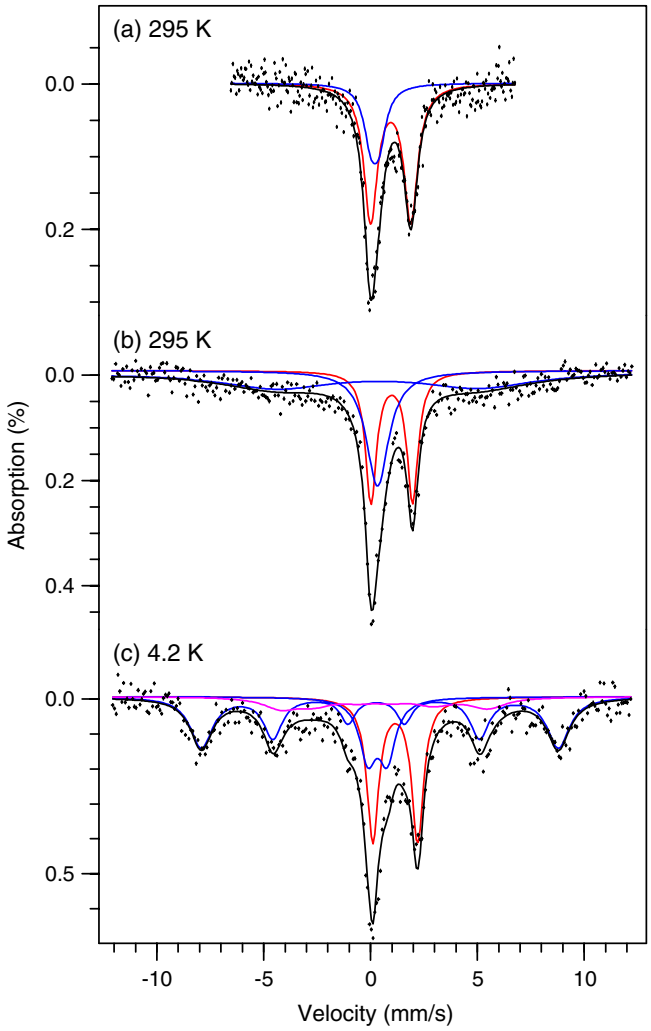

Figure 4. ^{57}Fe Mössbauer spectra of float composition glass containing 0.32 mol% Fe_2O_3. Spectra (a) and (b) are taken at 295 K over different velocity ranges. Spectrum (c) is taken at 4.2 K [15].
(This figure is in colour only in the electronic version)

measurements on ternary stannosilicate glasses with alkali (Li, Na, K, Rb and Cs) [30] and alkaline earth (Mg, Ca and Sr) [31] modifiers. Spectra of float glass were obtained by Principi *et al* using CEMS [32], by Johnson *et al* [29] using transmission Mössbauer spectroscopy (TMS) and by Williams *et al* [33] both by CEMS and TMS. Johnson *et al* [29] also studied tin-doped float glass with up to 6 mol% SnO. Tinted float glass containing a few mol% of added Fe_2O_3 was analysed by Williams *et al* [16, 17]. By using sectioned specimens, Williams *et al* [34] measured the spectra as a function of depth from the surface (see section 6).

5.1. Binary and ternary stannosilicates

The Mössbauer spectra of a series of binary stannosilicates are shown in figure 5 [28], and those of the ternary glasses are similar [30, 31]. The lines were broad, with a width greater

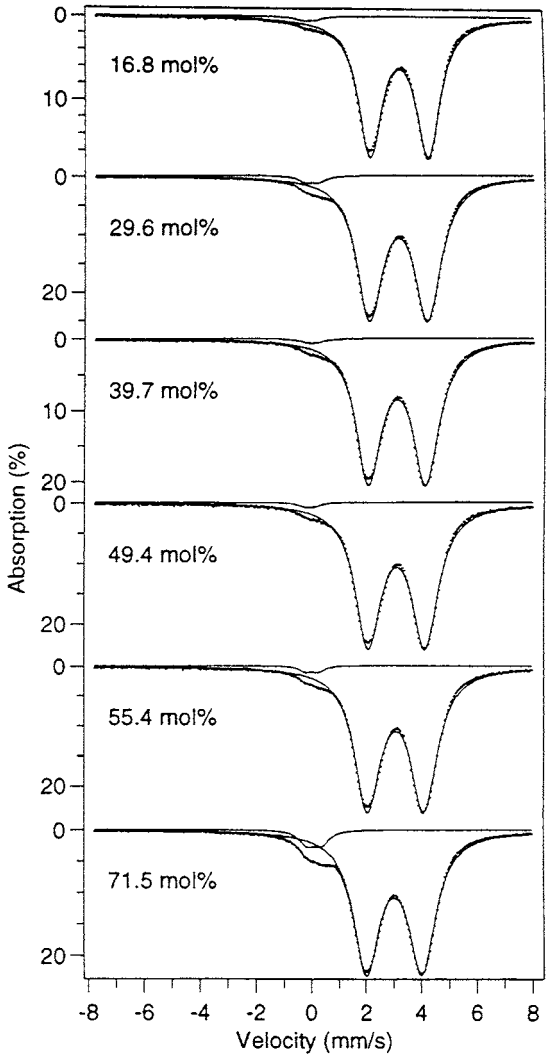

Figure 5. Mössbauer spectra at 77 K of ^{119}Sn in binary $(SiO_2)_{1-x}(SnO)_x$ glasses. The velocity is relative to $CaSnO_3$ at room temperature [28].

than 1 mm s^{-1} compared with the natural value of 0.4 mm s^{-1}, reflecting the large number of different sites in a disordered material. Narrower linewidths and better fits to the spectra could be obtained by fitting two components with slightly different shifts and quadrupole splittings, reinforcing the assumption that many sites exist. However, it was not generally possible to get consistent values of the fitted parameters over the whole range of composition and temperature. Hence, the spectra are usually fitted as broad quadrupole doublets, and the values of the shifts and quadrupole splittings quoted are averages.

Both Sn^{2+} and Sn^{4+} are present and are identified by their different isomer shifts and quadrupole splittings. Sn^{4+} has an isomer shift close to zero relative to a $CaSnO_3$ source and a small quadrupole splitting, whereas Sn^{2+} has a shift of 2–3 mm s^{-1} and a quadrupole splitting of 1–2 mm s^{-1}. The fraction of tin in the Sn^{4+} state generally increased with modifier concentration up to a value of about 10%. Tables 2 and 3 summarize the shifts δ (relative to

Table 2. Shifts (δ) in mm s^{-1} of ^{119}Sn in silicate glasses and inorganic oxides measured at 77 K relative to a $CaSnO_3$ source.

	Sn^{2+}	Sn^{4+}	Ref.
$(SiO_2)_{0.500}(SnO)_{0.400}(Al_2O_3)_{0.100}$	3.17	—	[31]
$(SiO_2)_{0.999}(SnO)_{0.001}$	3.11	−0.22	[28]
$(SiO_2)_{0.674}(SnO)_{0.326}$	3.06	−0.14	[28]
$(SiO_2)_{0.465}(SnO)_{0.535}$	2.98	−0.09	[28]
a-SnO	2.92[a]	—	[25]
a-SnO_2	—	0.13[a]	[25]
$(SiO_2)_{0.518}(SnO)_{0.344}(MgO)_{0.138}$	3	—	[31]
$(SiO_2)_{0.503}(SnO)_{0.298}(CaO)_{0.189}$	2.94	−0.28	[31]
$(SiO_2)_{0.500}(SnO)_{0.345}(SrO)_{0.150}$	2.91	−0.25	[31]
$(SiO_2)_{0.500}(SnO)_{0.450}(Cs_2O)_{0.050}$	2.95	—	[31]
Tin-doped float glass (6% Sn)	2.87	−0.2	[29]
Float glass[b]	2.84	−0.21	[34, 33]
Tinted float glass (2% Fe)	2.87	−0.2	[16]
$(SiO_2)_{0.547}(SnO)_{0.228}(Li_2O)_{0.209}$	2.86	−0.17	[30]
$(SiO_2)_{0.498}(SnO)_{0.275}(Na_2O)_{0.215}$	2.73	−0.19	[30]
$(SiO_2)_{0.559}(SnO)_{0.198}(K_2O)_{0.185}$	2.58	−0.14	[30]
$(SiO_2)_{0.559}(SnO)_{0.260}(Rb_2O)_{0.181}$	2.58	—	[30]
SnO	2.7	—	[25]
SnO_2	—	0.02	[25]

[a] Extrapolated from room temperature measurements.
[b] Typical float glass is $(SiO_2)_{0.73}(Na_2O)_{0.11}(CaO)_{0.08}(MgO)_{0.06}(Al_2O_3)_{0.01}(Fe_2O_3)_{0.01}$ with a trace of SnO at the surface.

Table 3. Quadrupole splittings (Δ) in mm s^{-1} of ^{119}Sn in silicate glasses and inorganic oxides measured at 77 K.

	Sn^{2+}	Sn^{4+}	Ref.
$(SiO_2)_{0.500}(SnO)_{0.400}(Al_2O_3)_{0.100}$	2.05	—	[31]
$(SiO_2)_{0.999}(SnO)_{0.001}$	2.12	0.42	[28]
$(SiO_2)_{0.674}(SnO)_{0.326}$	2.06	0.44	[28]
$(SiO_2)_{0.465}(SnO)_{0.535}$	2.05	0.47	[28]
a-SnO	1.71	—	[25]
a-SnO_2	—	0.7	[25]
$(SiO_2)_{0.500}(SnO)_{0.450}(Cs_2O)_{0.050}$	2.1	—	[31]
$(SiO_2)_{0.518}(SnO)_{0.344}(MgO)_{0.138}$	2.07	—	[31]
$(SiO_2)_{0.503}(SnO)_{0.298}(CaO)_{0.189}$	2.02	0.63	[31]
$(SiO_2)_{0.500}(SnO)_{0.345}(SrO)_{0.150}$	2.02	0.46	[31]
$(SiO_2)_{0.547}(SnO)_{0.228}(Li_2O)_{0.209}$	1.98	0.42	[30]
$(SiO_2)_{0.498}(SnO)_{0.275}(Na_2O)_{0.215}$	1.97	0.39	[30]
$(SiO_2)_{0.559}(SnO)_{0.242}(K_2O)_{0.199}$	1.93	—	[30]
$(SiO_2)_{0.559}(SnO)_{0.260}(Rb_2O)_{0.181}$	1.95	—	[30]
Tin-doped float glass	1.96	0.47	[29]
Float glass[a]	1.96	0.44	[34, 33]
Tinted float glass	1.97	0.43	[16]
SnO	1.36	—	[25]
SnO_2	—	0.5	[25]

[a] $(SiO_2)_{0.73}(Na_2O)_{0.11}(CaO)_{0.08}(MgO)_{0.06}(Al_2O_3)_{0.01}(Fe_2O_3)_{0.01}$.

the $CaSnO_3$ source) and quadrupole splittings Δ, respectively, for Sn^{2+} and Sn^{4+} measured at 77 K.

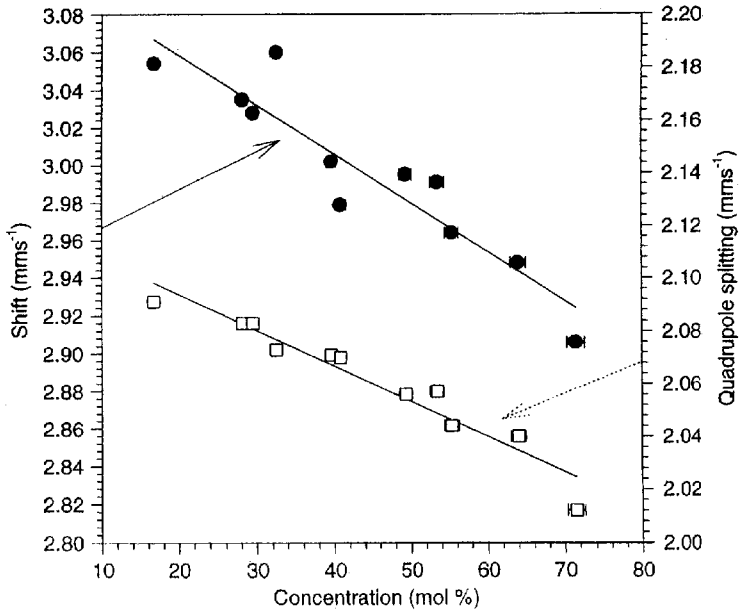

Figure 6. The variation of the average centre shift δ (●) and quadrupole splitting Δ (■) of Sn^{2+} in $SiO_2{\cdot}SnO$ at 77 K with SnO concentration [28].

The isomer shifts are consistent with the configurations $5s^2$ and $5s^0$ for ionic Sn^{2+} and Sn^{4+} respectively, giving Sn^{2+} the more positive shift of around 3 mm s^{-1} compared to that of Sn^{4+}, which has essentially no shift. For Sn^{2+}, which has non-bonding 5s electrons, the effect of covalency is to reduce the number of s electrons, i.e. to decrease the shift; for example, SnI_2 has a more negative shift than $SnCl_2$. The isomer shift for tetrahedrally co-ordinated Sn^{2+} is more negative than that for octahedral co-ordination. For Sn^{4+}, which has no electrons in the 5s shell, the isomer shift increases with increasing covalency; the stannic tetrahalides, which have the cations tetrahedrally co-ordinated to the tin, have a more positive isomer shift than the corresponding octahedrally co-ordinated ions SnX_6^{2-}. Also, four-co-ordinate Sn^{4+} has a more positive shift than six co-ordinate. Thus these effects for Sn^{4+} go in the opposite direction to those for Sn^{2+}.

For Sn^{2+} in the binary SiO_2–SnO series (no alkali modifier) the isomer shift tended to a value of 3.11 mm s^{-1} at 77 K for zero concentration of SnO. This shift is greater than that of amorphous SnO (2.92 mm s^{-1} [25]) and crystalline SnO (2.70 mm s^{-1} [25]). The shifts decreased with increasing tin content to a value close to that of amorphous SnO, as shown in figure 6. By contrast, the shifts and quadrupole splittings for Sn^{4+} increase with increasing tin content as expected, and are shown in figure 7.

The variation of the centre shift of Sn^{2+} for different modifier atoms substituted for tin in the almost equiatomic glass $(SiO_2)_{0.55}(SnO)_{0.45}$ is plotted in figure 8 and the quadrupole splittings are plotted in figure 9. For ternary stannosilicate glasses, the shift increases when Al_2O_3 is added, the largest value observed being 3.17 mm s^{-1} for 10% of the modifier. For alkaline earth modifiers Mg, Ca and Sr, the shift decreases slightly and is approximately linear with concentration [31]. Larger decreases are produced by the alkali modifier cations Na, K and Rb [30] (though Li shows a slight increase). The changes are largest for the heaviest atoms, the lowest value observed being 2.58 mm s^{-1} for 18% Rb_2O. The changes in quadrupole splittings are similar.

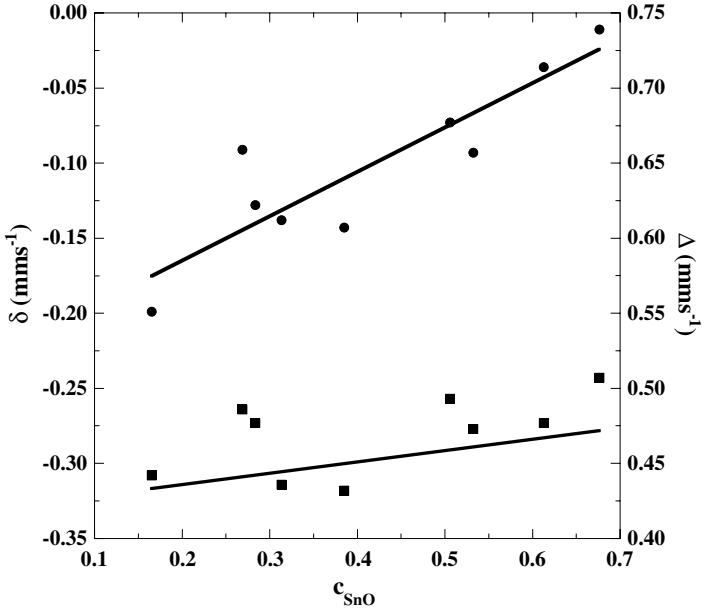

Figure 7. The variation of the average centre shift δ (●) and quadrupole splitting Δ (■) of Sn^{4+} in SiO_2·SnO at 77 K with SnO concentration [31].

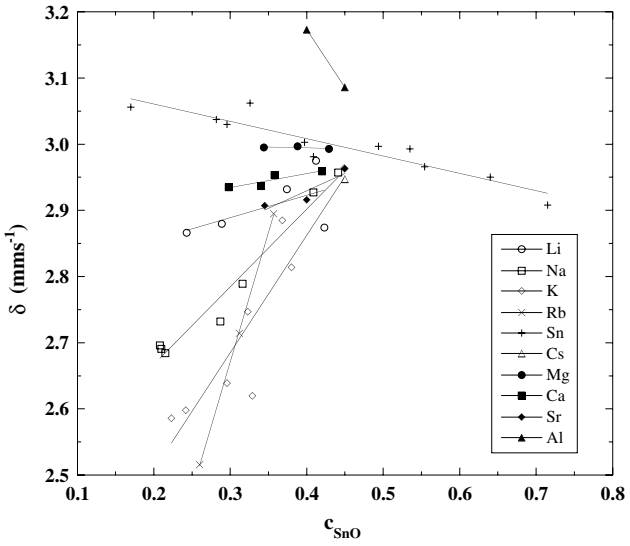

Figure 8. Sn^{2+} shifts at 77 K as a function of SnO concentration for ternary stannosilicate glasses [30, 31]. Data for the binary glasses (from figure 5) are shown for comparison.

The value of the isomer shift δ^{I} may be separated from the second-order Doppler shift δ^{SOD} by measuring the temperature dependence of the centre shift δ. As the temperature is increased δ^{SOD} decreases and may be calculated from equations (2) and (3). Since $\Delta\langle R^2\rangle$ is positive for ^{119}Sn, an increase in the isomer shift, equation (5), corresponds to an increase in electron density $|\psi_{\mathrm{s}}(0)|^2$ at the nuclei, i.e. $\partial\delta^{\mathrm{I}}/\partial \ln V$ is negative. So thermal expansion would

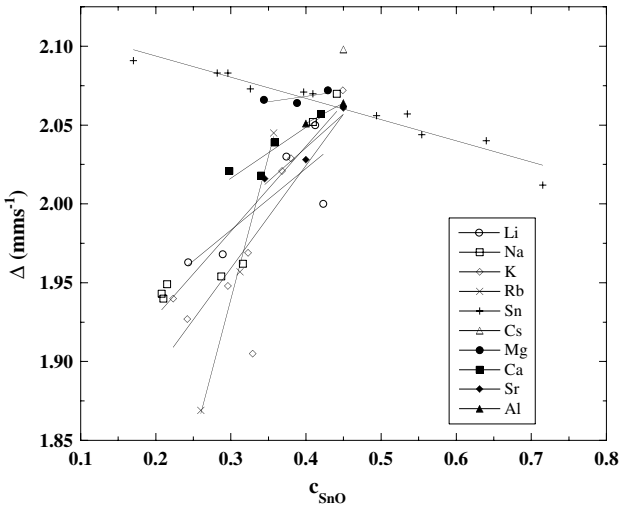

Figure 9. Sn^{2+} quadrupole splitting at 77 K as a function of SnO concentration for ternary stannosilicate glasses [30, 31]. Data for the binary glasses (from figure 5) are shown for comparison.

cause δ^{I} to decrease with increasing temperature according to

$$\frac{\partial \delta^{\mathrm{I}}}{\partial T} = \beta \frac{\partial \delta^{\mathrm{I}}}{\partial \ln V} \tag{14}$$

where β is the volume expansivity. At high temperatures ($T \gg \Theta_{\mathrm{D}}$) both δ^{SOD} and δ^{I} vary linearly with temperature, and a plot of δ against T should be a straight line. The predicted contribution to the slope from the second order Doppler shift according to equation (4) is $\partial\delta^{\mathrm{SOD}}/\partial T = -3.5 \times 10^{-4}$ mm s^{-1} K^{-1}, and the difference between this and the observed values must be due to the intrinsic temperature dependence of the isomer shift. An intrinsic temperature dependence of the ^{119}Sn isomer shift has previously been found in β-tin [35]. The slopes $\partial\delta/\partial T$ found for Sn^{2+} and Sn^{4+} in the binary and ternary stannosilicate glasses are given in table 4. In all cases the observed slope $\partial\delta/\partial T$ is negative and less steep than $\partial\delta^{\mathrm{SOD}}/\partial T$, and hence $\partial\delta^{\mathrm{I}}/\partial T$ is positive for the values given in the table. Figure 10 shows that the isomer shift δ^{I} increases with temperature while the centre shift, δ, decreases.

Although the consistency between the values of these slopes (table 4) is not good, partly owing to the variable amounts of tin and silicon present, they establish that an increase in δ^{I} implies an increase in molar volume and *vice versa*. This finding is in accord with pressure measurements on tin compounds [36], which generally show a decrease in shift when pressure is applied, i.e. when the density increases. The increase in electron density when the volume increases may be explained by the shielding effect of the tin p electrons. An increase in s-electron density could arise either from an increase in the number of s electrons in the region of the tin atoms, or from a decrease in the density of the p-electron orbitals of the tin, which shield the nuclei from the s electrons. In the present case the observed sign of the change in the shift indicates that they arise from changes in the p electrons, and not from covalent electron transfer.

Table 4 also gives the reduction of the quadrupole splitting $\partial\Delta/\partial T$ with temperature. Since the change in the angular term $\langle 3\cos^2\theta - 1\rangle$ in equation (7) is likely to be less than 20%, it follows from equation (8) that $\partial\Delta/\partial T = -\beta\Delta(0)$ at high temperatures. From the expansivities given in table 6, $\partial\Delta/\partial T$ would be expected to be of the order of 10^{-5} mm s^{-1} K^{-1} whereas

Table 4. Temperature dependence of the Mössbauer centre shift and the isomer shift for stannosilicate glasses $(SiO_2)_{0.5}(SnO)_{0.5-x}(RO)_x$ and $(SiO_2)_{0.5}(SnO)_{0.5-x}(M_2O)_x$ [28, 30, 31].

		Sn^{2+}			Sn^{4+}	
		$\partial\delta/\partial T$	$\partial\delta^{I}/\partial T$	$\partial\Delta/\partial T$	$\partial\delta/\partial T$	$\partial\delta^{I}/\partial T$
M	x	(10^{-4} mm s^{-1} K^{-1})	(10^{-4} mm s^{-1} K^{-1})	(10^{-4} mm s^{-1} K^{-1})	(10^{-4} mm s^{-1} K^{-1})	(10^{-4} mm s^{-1} K^{-1})
SnO	0.326	−2.73	0.760	−2.500	−2.38	1.12
MgO	0.138	−2.31	1.180	−2.390	—	—
CaO	0.151	−2.72	0.780	−2.760	—	—
SrO	0.15	−3.22	0.270	−2.870	—	—
Li_2-O	0.209	−2.63	0.861	−2.117	−2.43	1.07
Na_2O	0.245	−3.21	0.283	−2.410	−2.24	1.25
K_2O	0.185	−3.30	0.196	−2.266	−2.43	1.07
Rb_2O	0.181	−2.69	0.803	−2.850	—	—

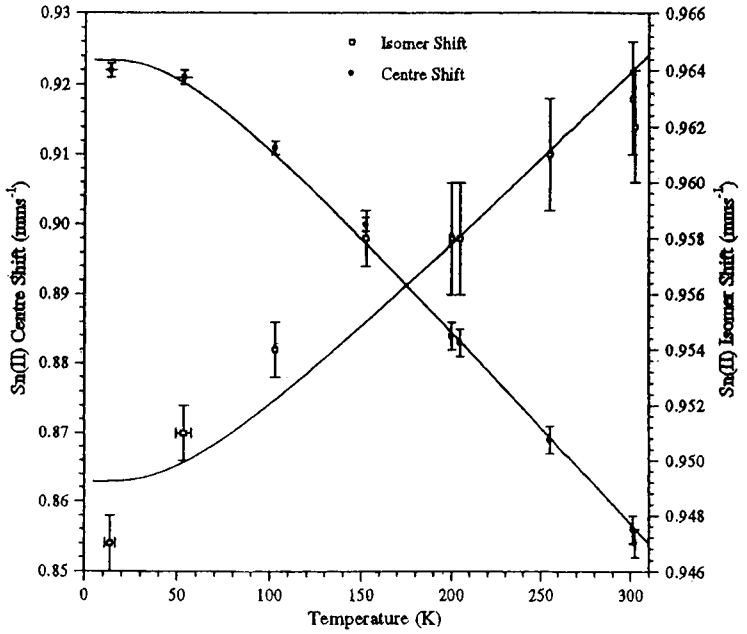

Figure 10. Variation of the centre shift δ and the isomer shift δ^{I} with temperature for the 50.6% binary stannosilicate glass [31].

Table 5. Change in isomer shift, molar volume and quadrupole splitting with the addition of modifier atoms and the volume corrected value [28, 30, 31].

	$\partial\delta^{\mathrm{I}}/\partial c_{\mathrm{M}}$ (10^{-2} mm s^{-1} mol^{-1})	$\partial V_{\mathrm{m}}/\partial c_{\mathrm{M}}$ (10^{-4} m^3 mol^{-1})	$\partial\delta^{\mathrm{I}}/\partial c_{\mathrm{M}}^{\mathrm{VC}}$ (10^{-2} mm s^{-1} mol^{-1})	$\partial\Delta/\partial c_{\mathrm{M}}$ (10^{-2} mm s^{-1} mol^{-1})
Al_2O_3	1.733	—	—	−0.269
SnO	−0.277	−0.035	—	−0.135
SnO_2	0.296	—	—	0.09
MgO	0.022	−0.073	—	−0.055
CaO	−0.197	−0.069	—	−0.294
SrO	−0.558	—	—	−0.459
Li_2O	−0.708	−0.121	−0.718	−0.505
Na_2O	−1.182	−0.013	−0.869	−0.52
K_2O	−2.099	0.1474	−1.77	−0.814
Rb_2O	−2.443	0.2866	−1.853	−0.867

the measured values are several times larger. This discrepancy again shows that changes in the p-electron density around the tin atoms are enhanced compared with the bulk density.

The variation in shift with tin concentration arises mainly from changes in δ^{I}, since (i) the volume dependence of δ^{SOD} is generally small [36] and (ii) the Debye temperatures do not vary greatly, and so the contribution from δ^{SOD} is about the same for all of the glasses. Values of $\partial\delta^{\mathrm{I}}/\partial c_{\mathrm{M}}$ are given in table 5, and are mostly negative. Table 5 also gives $\partial V_{\mathrm{m}}/\partial c_{\mathrm{M}}$ where V_{m} is the molar volume. As the molar volume increases, δ^{I} decreases, i.e. the electron density in the region of the tin nuclei increases proportionally to the size of the modifier ions.

The slope $\partial\delta^{\mathrm{I}}/\partial c_{\mathrm{M}}$ for each modifier is plotted against modifier radius in figure 11, and is seen to decrease with atomic size, and to increase with the valency of the modifier ion. For

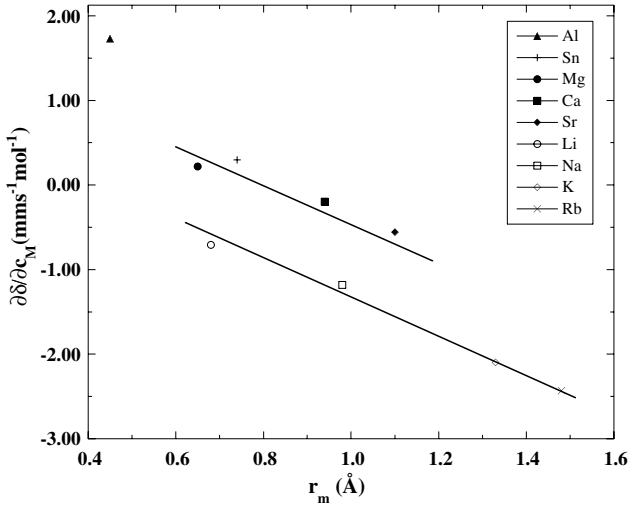

Figure 11. Rate of change of δ with modifier concentration as a function of modifier radius r_M [30]. The lines drawn through the alkali and alkaline earth modifier points are guides to the eye.

Table 6. Mean bond lengths and angles and coordination numbers of the ternary stannosilicate glasses $(SiO_2)_{0.5}(M_2O)_x(SnO)_{0.5-x}$ determined by neutron diffraction [30]. Errors on the bond lengths are ± 0.01 Å or better. Co-ordination numbers are much less accurate. Also shown are molar volumes V_m (from density measurements) and thermal expansivities β.

M	x	R_{Si-O} (Å)	C_{Si-O}	R_{Sn-O} (Å)	C_{Sn-O}	V_m (10^{-6} m^3)	β (10^{-5} K^{-1})	R_{O-O} (Å)	C_{O-O}	θ_{O-Sn-O}	θ_{O-Si-O}
Li	0.042	1.622	3.8	2.135	3.2	25.07	1.55	2.658	5.3	77	110
	0.086	1.623	3.6	2.133	3.2	24.03	1.9	2.663	5.1	77.3	110.2
	0.14	1.626	3.6	2.128	2.9	24.74	2.62	2.677	5.1	78	110.2
	0.167	1.625	3.6	2.137	3.3	23.32	2.95	2.672	5	77.4	110.6
	0.208	1.627	3.5	2.134	3	22.89	2.75	2.672	5.1	77.5	110.4
Na	0.049	1.626	3.6	2.119	3	26.25	—	2.645	5.7	77.2	108.8
	0.126	1.625	3.5	2.097	3.8	24.89	3	2.661	5.2	78.8	109.9
	0.204	1.629	3.5	2.089	4.1	25	—	2.666	5.1	79.3	109.8
	0.252	1.631	3.7	2.073	3.3	26.53	—	2.662	5.9	79.2	109.4
K	0.05	1.622	3.9	2.119	3.1	26.3	1.98	2.657	5.2	77.7	110
	0.097	1.625	3.7	2.103	3.1	26.83	2.95	2.651	5	78.1	109.3
	0.199	1.626	3.7	2.095	2.8	28.12	4.2	2.655	5	78.6	109.5
Rb	0.054	1.621	3.8	2.111	3.4	26.13	1.87	2.657	5	78	110.1
	0.124	1.624	3.6	2.089	3.3	29.17	3.06	2.666	5	79.3	110.3
	0.181	1.629	3.8	2.083	3.4	30.27	3.68	2.676	5.4	79.9	110.4

the monovalent alkali modifiers this observation agrees with structure determinations. The structure (mean bond lengths R_{X-O}, co-ordination numbers C_{X-O} and bond angles Θ_{O-X-O}) of the ternary alkali glasses has been studied by neutron diffraction by Johnson *et al* [30] and the results are given in table 6. Also shown in the table are molar volumes V_m (from density measurements) and thermal expansivities β. The tin is predominantly co-ordinated to three oxygen neighbours and generally the Sn–O bond lengths decrease and the O–Sn–O angles increase with increasing modifier concentration x, though the small changes in Li are in the

opposite direction. This reduction increases with increasing size of the modifier cation, and is opposite in sign to the macroscopic molar volume which increases with modifier content. As alkali atoms are added the [SiO_4] tetrahedra expand (both R_{Si-O} and R_{O-O} increase) and evidently exert pressure on the [SnO_3] units. At the extreme limits the large Rb^+ ion produces a large decrease in the ^{119}Sn isomer shift, while the small Al^{3+} ion increases it.

The change in isomer shift resulting from a change in volume may be estimated from the measured values of $\partial\delta^I/\partial T$, since

$$\left(\frac{\partial\delta^I}{\partial c_M}\right)_T = \frac{\kappa_c}{\beta}\left(\frac{\partial\delta^I}{\partial T}\right)_c \tag{15}$$

where

$$\kappa_c = \partial \ln V/\partial c_M \tag{16}$$

is the compressibility under changes in composition.

If the bulk molar volume V_m is used in equation (16), the correction given by equation (15) is negative. Since the local compressibility at the tin sites has the opposite sign from the bulk value, a more appropriate volume to use in κ_c would be the local one proportional to $(R_{SnO})^3$. This correction is given in table 5 together with the volume corrected value $\partial\delta^I/\partial c_M^{VC}$. The correction is not large but of the right sign, so that $\partial\delta^I/\partial c_M$ remains negative. The changes in δ^I are probably due solely to the changes in volume, but no independent measurement yields the appropriate volume to use in equation (16). Hence the change in isomer shift with both tin concentration or temperature may be explained in terms of the changes in molar volume, rather than from changes in co-ordination number or covalent electron transfer from neighbouring oxygen atoms.

The variation of f with temperature is shown in figure 12 for the 50.64% SnO binary glass fitted according to the Debye model. At absolute zero the values of f tend to 0.80 and 0.84 for Sn^{2+} and Sn^{4+} respectively, assuming the recoil energy E_R to be 2.572×10^{-3} eV.

The effective Debye temperatures Θ_D of Sn^{2+} and Sn^{4+} deduced from the decrease in the intensity of the spectra as the temperature was increased are given in table 7. In general they are larger for Sn^{4+} (∼220 K) than for Sn^{2+} (∼190 K), and decrease as the size of the modifier cation increases. The stronger bonding of Sn^{4+} is consistent with covalent bonds compared with the more ionic bonding of Sn^{2+}.

5.2. Float glass

Measurements on float glass have been made by CEMS [32] and TMS [29]. The measurements are difficult because of the small amount of tin concentrated at the surface. CEMS is sensitive to a depth of 2 μm, whereas transmission spectra sample the whole tin region of 10–20 μm. For transmission measurements the absorbers were specially prepared by grinding away the bulk glass, and several of these thinned specimens were stacked on top of each other.

Float glass has a variable composition, but glasses from different production lines exhibit fairly similar spectra. The majority of the tin is in the Sn^{2+} state, but there is considerably more Sn^{4+} than in the binary and ternary stannosilicate glasses, with fractions as much as 50% found in the oxidized state. The linewidths were similar to those found in binary and ternary stannosilicate glasses. The shifts were found to be 2.84 mm s^{-1} for Sn^{2+} and −0.21 for Sn^{4+}, with different specimens showing only small deviations from these values. For Sn^{2+}, taking the data for the shifts produced by different modifiers from figure 8 and assuming that the reductions in shift for each element (11% Na, 8% Ca, 6% Mg) are additive, there is agreement with the observed shift for float glass if the average concentration of tin in the top

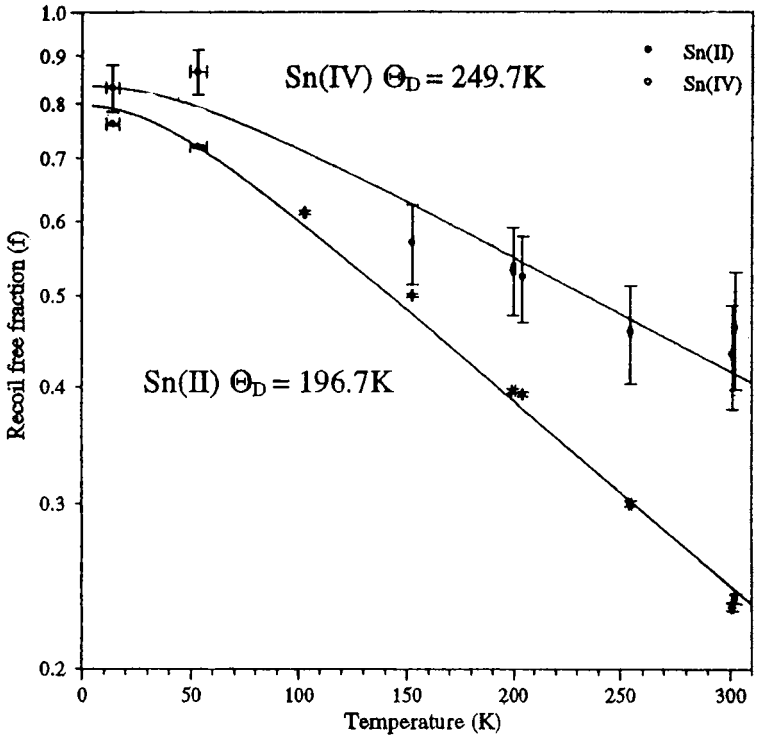

Figure 12. Variation of the recoil-free fractions f of Sn^{2+} and Sn^{4+} with temperature for the 50.4% SnO binary stannosilicate glass [31].

Table 7. Measured values of the effective Debye Θ of Sn^{2+} and Sn^{4+} in silicate glasses.

Θ_D	Sn^{2+}	Sn^{4+}	Ref.
$(SiO_2)_{0.500}(SnO)_{0.400}(Al_2O_3)_{0.100}$	188	—	[31]
$(SiO_2)_{0.999}(SnO)_{0.001}$	—	—	[28]
$(SiO_2)_{0.674}(SnO)_{0.326}$	191	209	[28]
$(SiO_2)_{0.465}(SnO)_{0.535}$	181	249	[28]
$(SiO_2)_{0.518}(SnO)_{0.344}(MgO)_{0.138}$	191	—	[31]
$(SiO_2)_{0.503}(SnO)_{0.298}(CaO)_{0.189}$	196	222	[31]
$(SiO_2)_{0.500}(SnO)_{0.345}(SrO)_{0.150}$	196	209	[31]
Tin-doped float glass	200	319	[29]
Float glass	185	260	[34, 33]
Tinted float glass	—	—	[16]
$(SiO_2)_{0.547}(SnO)_{0.228}(Li_2O)_{0.209}$	205	243	[30]
$(SiO_2)_{0.498}(SnO)_{0.275}(Na_2O)_{0.215}$	186	222	[30]
$(SiO_2)_{0.559}(SnO)_{0.242}(K_2O)_{0.199}$	183	287	[30]
$(SiO_2)_{0.559}(SnO)_{0.260}(Rb_2O)_{0.181}$	173	—	[30]
$(SiO_2)_{0.500}(SnO)_{0.450}(Cs_2O)_{0.050}$	175	—	[31]
SnO	203	—	[25]
SnO_2	—	313	[25]

surface is between 15 and 20%. The quadrupole splittings predicted in the same way from the stannosilicate data of figure 9 gave a value slightly above the 1.96 mm s^{-1} for float glass.

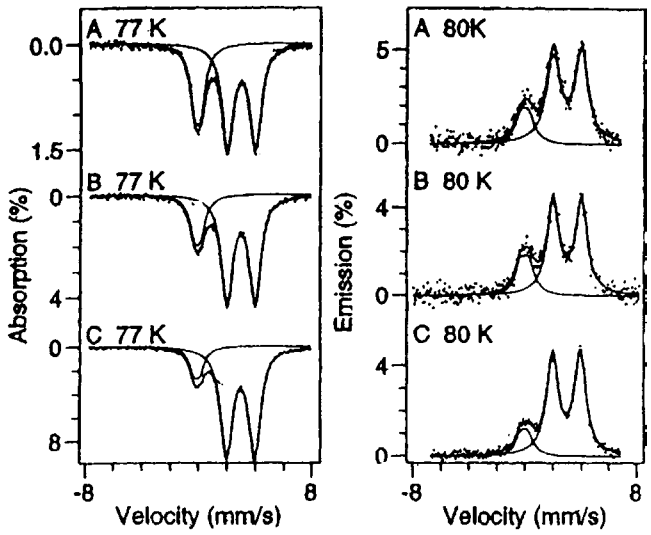

Figure 13. Transmission (total tin) and conversion electron (surface region) ^{119}Sn Mössbauer spectra of three float glass specimens [33] at 77 K. Note there is less Sn^{4+} at the surface.

The value of Θ_D for Sn^{2+} (185 K) was close to those found in the stannosilicate glasses, while Sn^{4+} gave somewhat higher values, 260 K compared with 220 K in the other glasses.

5.3. Float glass surface

Conversion electron and transmission spectra of float glasses are compared in figure 13 [33]. For Sn^{2+} the difference between atoms at the surface and the whole tin region is small. However, there is less Sn^{4+} at the surface compared with that in the whole tin layer, and the isomer shifts are more positive (-0.14 compared with -0.20 mm s^{-1}), and the quadrupole splittings are larger (0.55 compared with 0.41 mm s^{-1}). Also the effective Debye temperatures are lower (230 K compared with 260 K), hence Sn^{4+} very close to the surface is less tightly bound than that in the whole tin layer.

5.4. Tin-doped float glass

Johnson *et al* [29] obtained Mössbauer spectra of float glass remelted in air with between 3 and 15% by weight (1–6 mol%) of SnO added to it. These samples were allowed to come to room-temperature equilibrium in a crucible rather than the tin being diffused into the glass while it is travelling over the float bath. Hence most of the tin was uniformly distributed in the bulk of the glass, in contrast to float glass where it is in high concentration at the surface. For low concentrations practically all of the tin was oxidized to Sn^{4+} in the remelting process. As the total tin concentration increased the ratio of Sn^{2+} to Sn^{4+} increased, as can be deduced from the spectra in figure 14. This behaviour could be due to the solubility limit of Sn^{4+} in the glass.

The results were different from those obtained from the binary, ternary and float glasses. Overall the state of Sn^{2+} was similar to that found in float glass, but the value of the shift for Sn^{2+} is consistently slightly higher than for untreated float glass, 2.87 mm s^{-1} compared to 2.84 mm s^{-1}. This is in accord with the lower concentration of tin in the doped (bulk) samples.

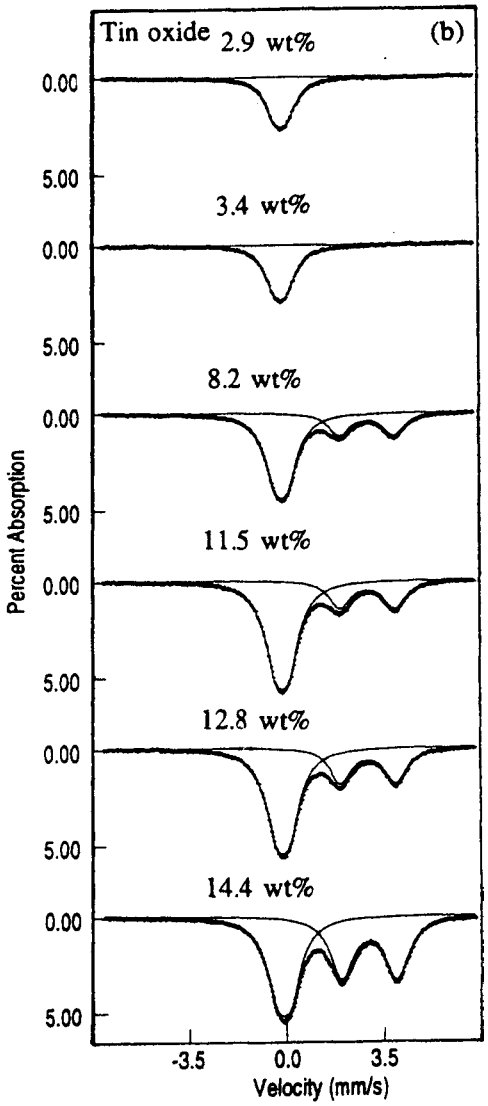

Figure 14. Mössbauer spectra at 77 K of ^{119}Sn in re-melted float glass for various concentrations of added SnO [29].

It is clear that the isomer shifts of tin in these glasses are very sensitive to composition. The Sn^{2+} shift decreased slightly with increasing tin concentration while that of Sn^{4+} increased, similar to the behaviour found in the binary SiO_2–SnO glasses [28]. The quadrupole splittings exhibit the same tendency. The linewidths showed the same broadening as that in all the other glasses studied.

There is a large difference between the binding in the two oxidation states in the tin-doped glass which is clear from the spectra measured at temperatures varying from 17.5 to 900 K shown in figure 15. The disappearance of the Sn^{2+} spectrum at 900 K is due to the smaller f-factor, not to oxidation to Sn^{4+}; on cooling back to room temperature its spectrum re-appeared. The value of Θ_D for Sn^{2+} was $\sim$200 K and that for Sn^{4+} $\sim$ 319 K. So the binding

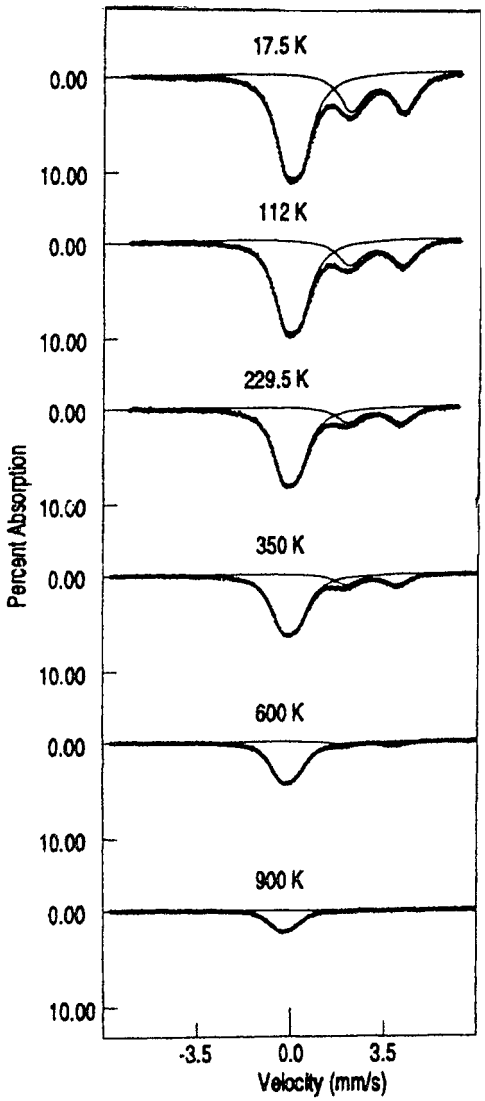

Figure 15. Mössbauer spectra at temperatures between 17.5 and 900 K of ^{119}Sn in re-melted float glass containing 6% (15% by weight) of added SnO [29].

strength, especially for Sn^{4+}, was significantly greater than that in float glass, indicating a weaker binding at the surface.

5.5. Tinted float glass

Measurements have been made by Williams *et al* [16, 17] on tinted float glass, which contains up to 2% Fe_2O_3. The shifts and quadrupole splittings are included in tables 2 and 3 and were close to those of clear float glass.

The fractions of Sn^{4+} deduced from the spectra increased with the amount of iron in the glass, and the interactions between the iron and tin will be further discussed in section 7.

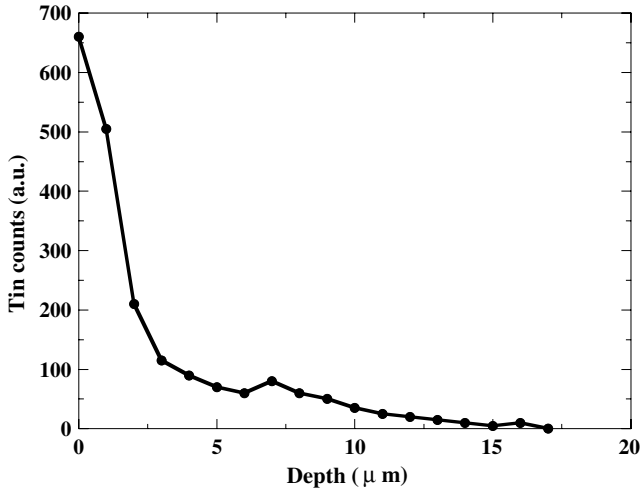

Figure 16. Depth profile of the total tin concentration in the lower surface of a float glass specimen determined by EMPA [34].

6. Measurement of the Sn^{2+} and Sn^{4+} depth profiles at the bottom float glass surface

The amount of each tin oxidation state present as a function of the depth from the float glass surface has been separately determined from their relative contributions to the Mössbauer spectrum [34].

Tin penetrates the bottom surface to a depth of about 20 μm, depending upon the particular plant in which it was made. Sieger [37], using electron microprobe analysis (EMPA), was the first to observe a buried maximum in the total tin concentration from about 5 to 10 μm, depending on the glass thickness, i.e. the time the glass spends in contact with the molten tin. Subsequent measurements by EMPA, ion beam analysis [38, 39], cathodoluminescence [40] and refractive index of the surface layer deduced from waveguide mode analysis [40] have confirmed this observation in many, though not all, samples. The profile is sensitive to the conditions under which the glass is made. The results obtained by different techniques have been compared by Townsend *et al* [41].

None of these methods distinguished the oxidation states of the tin, whereas the Mössbauer effect can. Since the float glass process is performed in a reducing atmosphere, it is expected that Sn^{2+} is present at the surface, but may become oxidized as it diffuses into the glass.

Williams *et al* [34] measured the ^{119}Sn Mössbauer spectra of a series of float glass specimens in which successive thicknesses of the lower surface (i.e. the surface in contact with the molten tin) had been removed by polishing. Ideally the removed glass should have been measured, but this was not practical. Instead the glass was first ground down to a thickness of 0.1 mm so that 23.6 keV γ-rays could be transmitted, and as the surface was polished away the spectrum averaged over the deeper layers containing less and less tin was measured. The Sn^{4+}/Sn^{2+} ratio was determined for each specimen, and corrected for the different f-values (0.86 for Sn^{4+} and 0.68 for Sn^{2+}).

The electron microprobe analysis (EMPA) data for the sample are shown in figure 16, giving a maximum at a depth of about 7 μm. The Mössbauer spectra are shown in figure 17. It was found that averaged over the whole 17 μm depth (figure 17(a)) 20% of the tin was in the Sn^{4+} state. As the surface was polished away this fraction increased (figure 17(d)) to 36% for

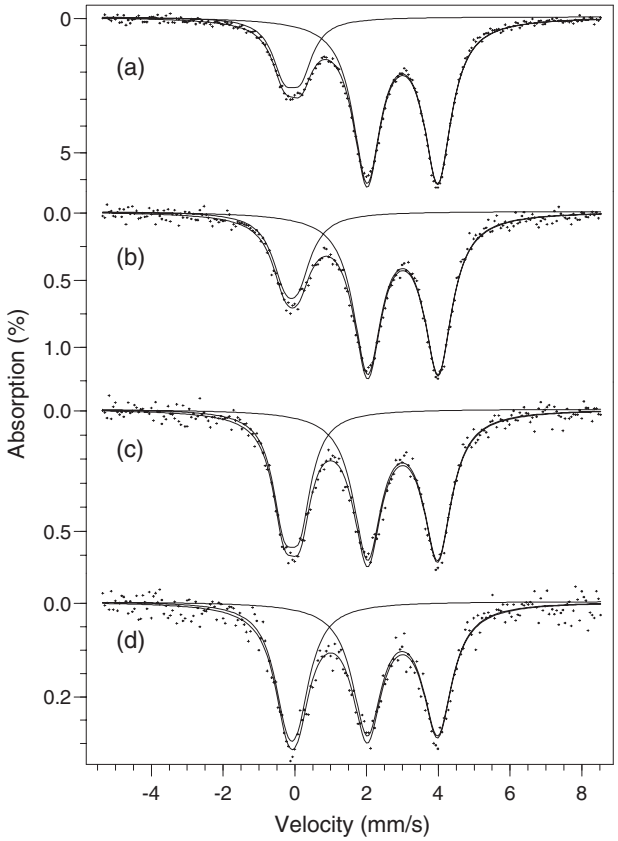

Figure 17. Mössbauer spectra at 77 K of ^{119}Sn ion of a float glass sample containing tin to a depth of (a) 17 μm and the same sample with a further (b) 1.5 μm (c) 3.5 μm and (d) 7.5 μm removed [34].

the uppermost region between 7.5 and 17 μm, i.e. the region beyond the maximum in the profile. The fraction of the tin in each oxidation state for the 3.5–7.5 μm layer (figure 17(c)), which could not be measured directly, was obtained by subtraction. These results were combined with the total tin profile to yield the variation of the Sn^{2+} and Sn^{4+} concentrations with depth, relative to a value of 100% for Sn^{2+} at the glass–tin interface (figure 18). The data show that the majority of the tin nearest the surface exists as Sn^{2+}, about 60% of which occurs in the first 3.5 μm. This value falls off rapidly with increasing depth. By contrast the concentration of Sn^{4+}, which is only a few per cent of that of Sn^{2+} at the surface, varies much more slowly. About 80% of Sn^{4+} is at a depth greater than 3.5 μm, and below 8 μm most of the tin is in the 4+ state.

7. Interactions between tin and iron in the surface layer of float glass

Williams *et al* [16, 17] studied the interaction between tin and iron in the float glass surface by measuring both ^{57}Fe and ^{119}Sn Mössbauer spectra in the same specimens. Verità *et al* [38, 39] had previously shown by EMPA, secondary ion mass spectrometry and other techniques that the iron concentration near the surface of float glass is different from that in the underlying bulk. Its profile shows a minimum at about the depth that the tin shows a maximum.

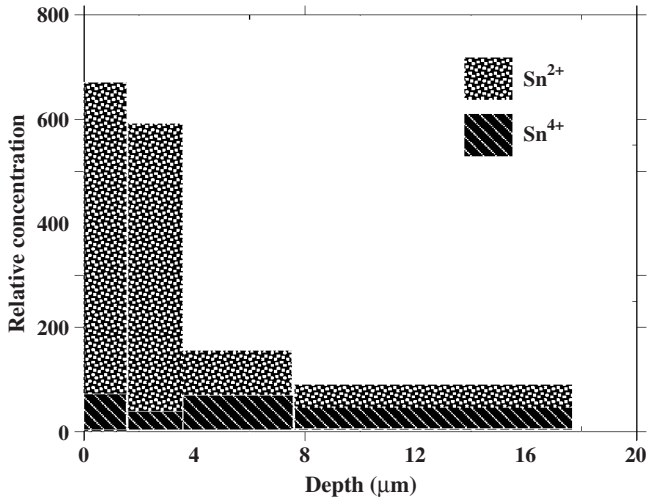

Figure 18. Histogram of the depth profiles of the Sn^{2+} and Sn^{4+} concentrations in a float glass surface determined from Mössbauer spectra [34].

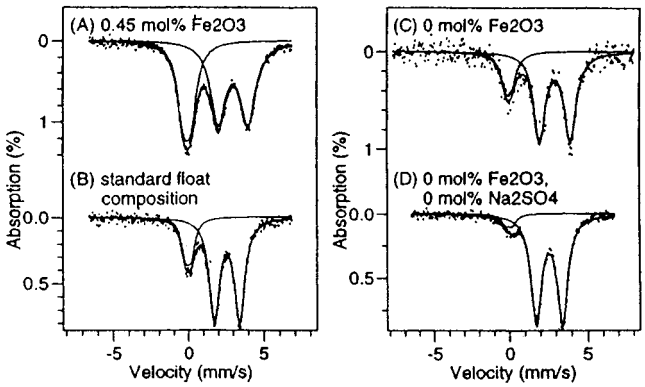

Figure 19. ^{119}Sn Mössbauer spectra at 77 K of (a) tinted float glass with 0.45 mol% Fe_2O_3, (b) standard float glass (0.04 mol% Fe_2O_3), (c) float glass made from iron-free silica and (d) iron-free float glass made without sodium modifier [17].

Mössbauer measurements [17] were made on surface and bulk samples. The surface samples comprised stacks of specimens, each prepared from the first 100 μm of the bottom surface. The remaining glass made up the bulk specimens and contained virtually no tin. The samples were prepared from iron-free silica and contained between 0 and 0.45 mol% Fe_2O_3. One of them contained no alkali modifier (sodium sulfate, Na_2SO_4) to study its effect on the oxidation state of the tin. The ^{119}Sn Mössbauer spectra for different iron concentrations are shown in figure 19 [17]. The $Sn^{4+}/(Sn^{4+} + Sn^{2+})$ fraction is low (about 7%) for the iron- and sodium-free glass (figure 19(d)). When sodium modifier is added it increases to about 20%. As the iron concentration is increased the oxidation of the tin increases to over 40% for the glass containing the most iron (figure 19(a)). Thus the fraction of Sn^{4+} increases with the amount of iron in the glass.

The ^{57}Fe Mössbauer spectra of the surface and bulk regions are compared in figure 20 [16], and show that the concentration of Fe^{2+} in the surface is higher than in the bulk. The amount

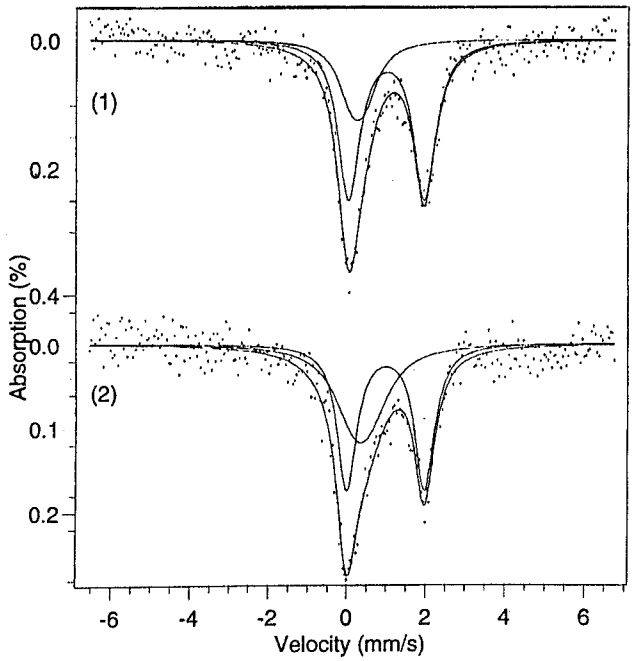

Figure 20. ^{57}Fe Mössbauer spectra of (1) surface and (2) bulk regions of dark green (0.38 mol% Fe_2O_3) glass [16] showing an increase in Fe^{2+} at the surface.

of Fe^{2+} produced by the reduction of Fe^{3+} increases as the iron content is increased, i.e. as the Sn^{2+} is reduced. Typical values for Fe^{2+} in the bulk are 64% for the lower iron concentration compared to 73% for the higher iron concentration. A similar trend is found for the surface spectra, which also showed consistently more Fe^{2+} than bulk samples of the same composition.

These data suggest that the iron oxidizes the tin in the surface region of float glass according to the reaction

$$Sn^{2+} + Fe^{3+} \rightarrow Sn^{4+} + Fe^{2+}.$$

In addition CEMS was used to study the near-surface tin and iron [17]. CEMS samples tin to a depth about 2 μm and iron to 0.1 μm. Some spectra are shown in figure 21. Both oxidation states of tin and iron are present in the near-surface region, evidence for oxidation of tin by the iron in the float glass plant.

8. Heat treatment and oxidation

The oxidation of tin when glasses are heated in air has also been studied for binary glasses $(SiO_2)_{1-x}(SnO)_x$ [28] and float glass [32, 34] using Mössbauer spectroscopy. Williams *et al* [34] heated float glass in air for various times at various temperatures and then slowly cooled it. Figure 22 shows spectra for samples heated at 730 °C for various times and then cooled. The fractions of Sn^{4+} as a function of time and temperature are summarized in table 8, which indicates that the amount of Sn^{4+} increases to 100% after heating for 10 min at 1050 °C. From the fraction of Sn^{4+} present, the diffusivity of oxygen in float glass was estimated to vary from 1.29×10^{-18} m^2 s^{-1} at 500 °C to 1.92×10^{-16} m^2 s^{-1} at 730 °C. The data fit a law $D = D_0 e^{-\Delta/kT}$, where the activation energy $\Delta = 1.45$ eV and $D_0 = 3.3 \times 10^{-9}$ m^2 s^{-1}.

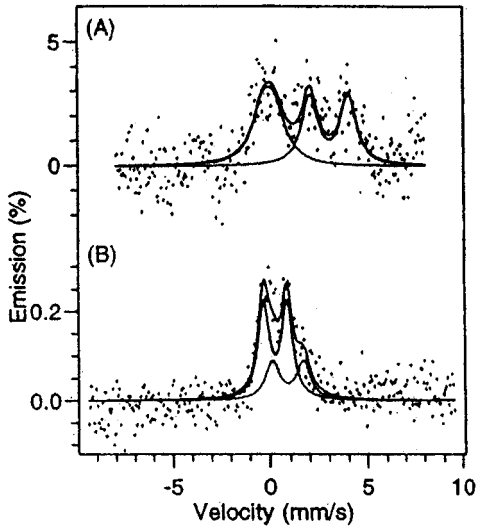

Figure 21. Conversion electron Mössbauer spectra of (a) ^{119}Sn and (b) ^{57}Fe in the near-surface region of float glass measured at room temperature [17].

Table 8. Fraction of Sn^{4+} and Debye Θ of Sn^{4+} and Sn^{2+} after heat treatment for various temperatures and times [34].

Float glass sample	Percentage Sn^{4+}	$\Theta_D(Sn^{4+})$ K	$\Theta_D(Sn^{2+})$ K
Unheated	20.6 ($\pm\leqslant$1%)	260 ($\pm$0.2)	185 ($\pm$0.1)
120 h at 500 °C	45.2 ($\pm\leqslant$1%)	258 ($\pm$0.4)	180 ($\pm$0.2)
2 h at 730 °C	55.3 ($\pm\leqslant$1%)	282 ($\pm$0.6)	187 ($\pm$0.4)
10 min at 1050 °C	100 ($\pm\leqslant$1%)	263 ($\pm$0.5)	—

The isomer shifts do not change appreciably on heating. The Debye temperature Θ_D for Sn^{4+} increases for heating up to the glass transition temperature ($T_g = 580\,°C$) but appears to fall again at higher temperatures where a more open structure is frozen in on cooling. When the glasses were heated in argon, there was no detectable increase in Sn^{4+}.

The presence of tin in the float glass surface and the variability of its oxidation state changes the physical properties (refractive index, thermal expansivity, viscosity, etc) and also the chemical properties. These differences can become significant during secondary processing such as chemical toughening or heat treatments. In particular, the wrinkling of the surface during heat treatment produces a greyish haze known as bloom. There is thus considerable technological interest in understanding how tin affects the various properties of float glass, and also scientific interest in establishing the specific structural changes brought about by the incorporation of tin. Williams *et al* [42] have studied bloom using Mössbauer spectroscopy. They found that the presence of iron in tinted glass reduced the amount of bloom. This reduction was attributed to the greater proportion of Sn^{4+} at the surface before heat treatment, as previously noted in section 7.

9. Conclusion

Most of the iron is in the Fe^{3+} state with fourfold co-ordination and effective Debye temperature $\Theta_D = 310$ K. Most of the tin is in the Sn^{2+} state, with an average co-ordination number of

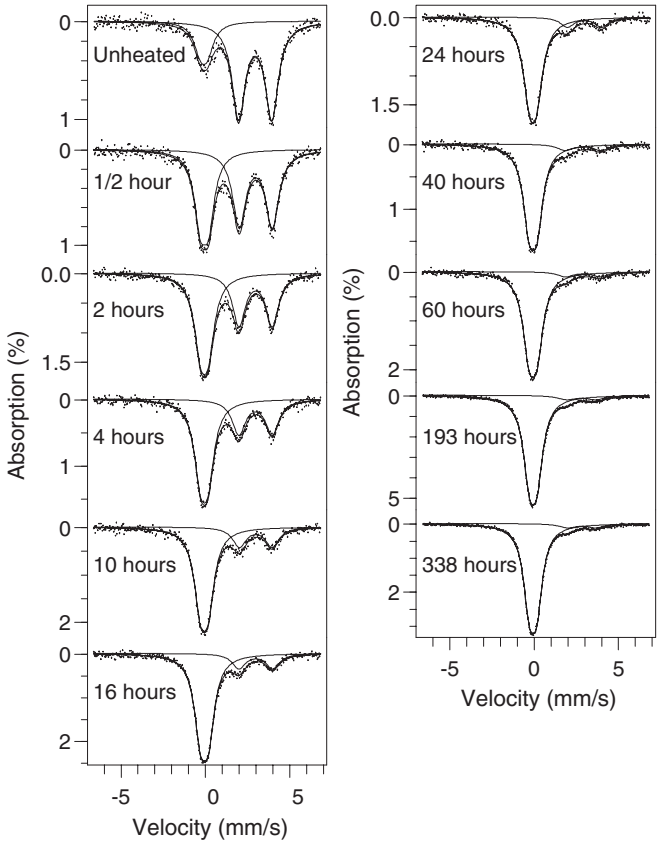

Figure 22. Mössbauer spectra at 77 K of ^{119}Sn in float glass which had been heated at 730 °C for various times up to 338 h and then cooled slowly [34].

four or less and a Θ_D of about 180 K. The minority Fe^{2+} and Sn^{4+} atoms are sixfold co-ordinated with $\Theta_D = 260$ K for Fe^{2+} and 220 K for Sn^{4+}. It appears that Sn^{2+} and Fe^{3+} act as conditional glass formers in silicates, while Sn^{4+} and Fe^{2+} are modifiers. The ^{119}Sn isomer shifts and quadrupole splittings of Sn^{2+} in simple binary and ternary silicate glasses containing an alkali or alkaline earth modifier decrease as the modifier content is increased. These changes correlate for each series with a reduction in the mean Sn–O bond lengths determined by neutron diffraction. Thus they are due to small changes in the local structure and atomic volume as the composition is varied, and these observations enable the shift observed in float glass and in tin-doped float glass to be understood. The reduction in shift increases with increasing size of the modifier cation and is opposite in sign to the macroscopic molar volume, which increases with greater modifier content. These results suggest that the modifier atoms exert pressure on the neighbouring Sn–O polyhedra.

Measurement of the relative areas of the Sn^{2+} and Sn^{4+} contributions to the Mössbauer spectrum of sectioned specimens enables the depth profiles of the two oxidation states to be determined separately. By monitoring the oxidation of Sn^{2+} to Sn^{4+} produced by heat treatment in air, the diffusion coefficient of oxygen was found to obey the law $D = D_0 e^{-\Delta/kT}$, with $\Delta = 1.45$ eV and $D_0 = 3.3 \times 10^{-9}$ m^2 s^{-1}. Measurements on tinted float glass show that the iron and tin react with each other, the Fe^{3+} oxidizing the Sn^{2+} to Sn^{4+}. A possible flow diagram is given of the chemical reactions in the float-glass process is given in figure 23 [17].

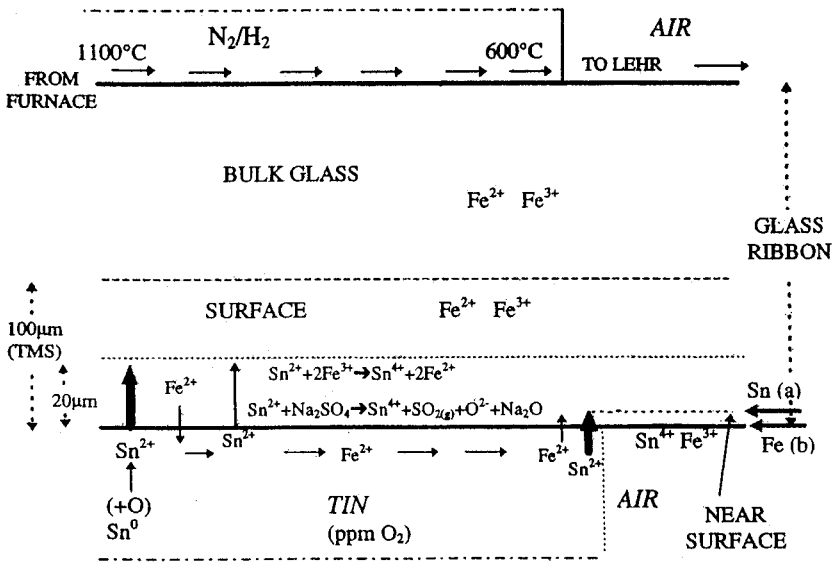

Figure 23. Illustration of the diffusion of tin and iron and their interactions in the float glass ribbon; the CEMS region is indicated for (a) tin and (b) iron to depths of 2 and 0.1 μm, respectively [17].

The literature on glass is vast, and we have confined ourselves in this article to silicate glasses and not attempted to review work on borate [43], germanate [44], chalcogenide [45] and oxychloride [46] glasses.

Acknowledgments

This work was supported by the US Department of Energy, Office of Science, under contract No W-31-109-ENG-38. We are also grateful to the EPSRC and the Leverhulme Foundation for support. We would like to thank our colleagues at Liverpool (Mike Thomas, Kyle Williams and Paul Appleyard), Warwick (Diane Holland), Argonne (David Price) and Pilkingtons (Jane Greengrass and Brian Tilley) for their valuable contributions.

References

[1] Elliott S R 1984 *The Physics of Amorphous Materials* (London: Longmans)
[2] Gaskell P 1995 *J. Non-Cryst. Solids* **192/193** 9
[3] Barker T C 1994 *An Age of Glass* (London: Boxtree) and conversation with Sir Alistair Pilkington
[4] Kirkjian C R 1970 *J. Non-Cryst. Solids* **3** 157
[5] Coey J M D 1974 *J. Physique Coll.* **12** C6 95
[6] Müller-Warmuth W and Eckert H 1982 *Phys. Rep.* **88** 93
[7] Tomandl G 1990 *Glass Science and Technology* vol 4B (New York: Academic) chapter 5
[8] Nishida T 1995 *Hyperfine Interact.* **95** 23
[9] Pollack H *et al* 1962 *The Mössbauer Effect* ed D M J Compton and A H Schoen (New York: Wiley) p 298
[10] Darby D M 1985 *Am. Mineral.* **70** 304
[11] Kurkjian C R and Buchanan D N E 1964 *Phys. Chem. Glasses* **5** 63
[12] Gosselin J P, Shimony U, Grodzins L and Cooper A R 1967 *Phys. Chem. Glasses* **8** 56
[13] Levy R A, Lupis C H P and Flynn P A 1976 *Phys. Chem. Glasses* **17** 94
[14] Johnson J A, Johnson C E, Holland D, Mekki A, Appleyard P and Thomas M F 1999 *J. Non-Cryst. Solids* **246** 104

[15] Williams K F E, Johnson C E and Thomas M F 1998 *J. Non-Cryst. Solids* **226** 19
[16] Williams K F E, Thomas M F, Johnson C E, Tilley B P, Greengrass J and Johnson J A 1997 Fundamentals of glass science and technology *Int. Conf. on Glass (Växjö, Sweden)* p 127
[17] Williams K F E, Thomas M F, Johnson C E, Johnson J A and Greengrass J 1999 *ICG 98: Proc. Int. Congress on Glass (San Francisco, July 1998)* vol B7, pp 29–35 (CD-ROM)
[18] Hayashi M, Hori M, Susa M, Fukuyama H and Nagata K 2000 *Phys. Chem. Glasses* **41** 49
[19] Bingham P A, Parker J M, Searle T, Williams J M and Fyles K 1999 *J. Non-Cryst. Solids* **253** 203
[20] Hirao K, Komatsu T and Soga N 1980 *J. Non-Cryst. Solids* **40** 315
[21] Ramachandran B E and Balasubramanian N 1986 *J. Mater. Sci. Lett.* **5** 1073
[22] Iwamoto N, Umesaki N and Atsumi T 1987 *J. Mater. Sci. Lett.* **6** 271
[23] Frischat G H and Tomandl G 1969 *Glastech. Ber.* **42** 182
[24] Mogus-Milankovic A, Long G J and Day D E 1995 *Phys. Chem. Glasses* **36** 31
[25] Collins G S, Kachnowski T, Benczer-Koller N and Pasternak M 1979 *Phys. Rev.* B **19** 1369
[26] Dannheim H, Oel H J and Tomandl G T 1976 *Glasstech. Ber.* **49** 170
[27] Mitrofanov K P and Siderov T A 1967 *Sov. Phys.—Solid State* **9** 693
[28] Williams K F E, Johnson C E, Johnson J A, Holland D and Karim M M 1995 *J. Phys.: Condens. Matter* **7** 9485
[29] Johnson J A, Johnson C E, Williams K F E, Holland D and Karim M M 1995 *Hyperfine Interact.* **95** 41
[30] Johnson J A, Johnson C E, Holland D, Sears A, Bent J F, Appleyard P G, Thomas M F and Hannon A C 2000 *J. Phys.: Condens. Matter* **12** 213–30
[31] Appleyard P G 2000 *PhD Thesis* Liverpool John Moores University, unpublished
[32] Principi G, Maddelena A, Gupta A, Geotti-Bianchini F, Hreglich S and Verita M 1993 *J. Nucl. Instrum. Methods* B **76** 215
[33] Williams K F E, Johnson C E, Nikolov O, Thomas M F, Johnson J A and Greengrass J 1998 *J. Non-Cryst. Solids* **242** 183–8
[34] Williams K F E, Johnson C E, Greengrass J, Tilley B P, Gelder D and Johnson J A 1997 *J. Non-Cryst. Solids* **211** 164
[35] Rothberg G M, Guimard S and Benczer-Koller N 1970 *Phys. Rev.* B **1** 136
[36] Williamson D L 1978 *Mössbauer Isomer Shifts* ed G K Shenoy and F E Wagner (Amsterdam: North-Holland) chapter 6b, p 317
[37] Sieger J S 1975 *J. Non-Cryst. Solids* **19** 213
[38] Verita M, Geotti-Bianchini F, Hreglich S, Pantano C G and Bojan V 1992 *Bol. Sociedad Española Ceramica y Vidru* C(6) **31** 415
[39] Verita M, Geotti-Bianchini F, Guadagnino E, Stella A, Pantano C G and Paulson T 1995 *Glastech. Ber.* **68** 251–8
[40] Yang B, Townsend P D and Holgate S A 1994 *J. Phys. D: Appl. Phys.* **27** 1757
[41] Townsend P D, Can N, Chandler P J, Farmery B W, Lopez-Heredoro R, Peto A, Salvin L, Underdown D and Yang B 1998 *J. Non-Cryst. Solids* **223** 73
[42] Williams K F E, Thomas M F, Greengrass J and Bradshaw J M 1999 *Glass Technol.* **40** 103
[43] Holland D, Hannon A C, Smith M E, Johnson C E, Thomas M F and Beesley A M 2004 *Solid State Nucl. Magn. Reson.* **26** 172
[44] Holland D, Smith M E, Poplett I J F, Johnson J A, Thomas M F and Bland J 2001 *J. Non-Cryst. Solids* **293–295** 175
[45] Boolchand P 2000 *Insulating and Semiconducting Glasses* ed P Boolchand (Singapore: World Scientific) p 191
[46] Johnson J A, Holland D, Bland J, Johnson C E and Thomas M F 2003 *J. Phys.: Condens. Matter* **15** 755